stresses

MDPI

Article

Dual-Mechanism Induced by 24-Epibrassinolide Synergistically Improves Anatomical Structures and the Antioxidant Defense System in Soybean Plants Under Cadmium Excess

Andreza Sousa Carmo [1], Ivan Becari Viana [2], Caroline Cristine Augusto [3], Bruno Lemos Batista [3] and Allan Klynger da Silva Lobato [1,*]

[1] Núcleo de Pesquisa Vegetal Básica e Aplicada, Universidade Federal Rural da Amazônia, Rodovia PA 256, Paragominas 68627-451, Pará, Brazil; carmo.andrezzas@gmail.com
[2] Departamento de Ciências Biológicas, Universidade do Estado de Minas Gerais—Unidade Carangola, Carangola 36800-000, Minas Gerais, Brazil; ivan.viana@uemg.br
[3] Centro de Ciências Naturais e Humanas, Universidade Federal do ABC, Santo André 09280-560, São Paulo, Brazil; caroline.c.augusto@gmail.com (C.C.A.); bruno.lemos@ufabc.edu.br (B.L.B.)
* Correspondence: allan.lobato@ufra.edu.br; Tel.: +55-91-993134006

Abstract

Cadmium (Cd) accumulation in plant tissues causes several damages, including disturbances in anatomical structures, negative impacts on photochemical reactions, and reducing the efficiency of the photosynthetic apparatus. 24-Epibrassinolide (EBR) is a plant steroid that regulates multiple physiological and biochemical processes to counteract the harmful effects of metal stress. The aim of this research was to investigate whether exogenous EBR application affects leaf and root anatomical structures, including stomatal responses, redox-metabolism-related biochemical responses intrinsically related to photosynthetic apparatus, and nutritional status in soybean plants under Cd excess. The experiment was randomized with four treatments: two cadmium concentrations (0 and 500 µM Cd, described as −Cd and +Cd, respectively) and two EBR levels (0 and 100 nM EBR, described as −EBR and +EBR, respectively). Results demonstrated that EBR positively regulated root and leaf structures and stomatal performance, with significant increases in epidermis and cortex (root) and benefits for spongy parenchyma and stomatal density (leaf), clearly protecting the photosynthetic apparatus against Cd excess. Simultaneously, this steroid mitigated Cd-induced oxidative stress by stimulating the activities of superoxide dismutase (25%), catalase (28%), ascorbate peroxidase (30%) and peroxidase (48%), while simultaneously reducing the content of oxidative compounds, including superoxide (16%), hydrogen peroxide (8%), malondialdehyde (12%) and electrolyte leakage (14%). The dual mechanism modulated by EBR protected anatomical structures and stimulated antioxidant defense. Therefore, the results prove that exogenous EBR application effectively attenuates the adverse effects of Cd excess in soybean plants.

Keywords: *Glycine max*; anatomy protective; brassinosteroids; photosynthetic apparatus; redox metabolism

Check for updates

Academic Editors: Yinbo Gan and Martin Backor

Received: 9 March 2026
Revised: 25 March 2026
Accepted: 8 April 2026
Published: 15 April 2026

Copyright: © 2026 by the authors. Licensee MDPI, Basel, Switzerland. This article is an open access article distributed under the terms and conditions of the Creative Commons Attribution (CC BY) license.

1. Introduction

Soybean [*Glycine max* (L.) Merrill] contributes more than 25% of global protein needs for human consumption and animal feed [1], playing an essential role in maintaining the sustainability of agricultural systems and global food security [2]. The crop adapts to a wide

range of climatic conditions and soil types, making it highly versatile, unlike traditional species such as corn, cotton, and sorghum [3]. The global soybean sector is worth US$155 billion and is projected to reach US$278 billion by 2031 [4,5]. In the last decade, the Brazilian soybean sector has expanded by 60%, and a further 30% increase in production is estimated by 2030, compared to 2020 [6].

The contamination of agricultural soils with heavy metals (HMs) has raised significant concerns due to increased bioavailability and accumulation of HMs in crops [7]. Cadmium (Cd) accumulation stems from natural activities, such as weathering, and anthropogenic factors [8], especially the development of agriculture and industries, representing a serious threat to human and animal health due to its high mobility [9]. As a highly mobile HM, Cd is easily absorbed by plants and translocated to the aerial parts, disrupting the physiological and metabolic processes of plants [10], maximizing ROS production, causing damage to the plant membrane through increased oxidative activity [11], and consequently reducing plant growth and productivity [12].

In plants, roots represent the first site of perception and impact from soil toxicity, where initial damage and the first defense responses occur [13,14], frequently promoting nutrient and pH imbalances, interfering with cellular processes and the physiological effects of plants [15]. On the other hand, anatomical adaptations of plant tissues exposed to heavy metal stress indicate potential strategies to mitigate their harmful effects [16,17], including modifications in root structures [18], such as inhibition of root growth and architecture due to reduced lateral root formation, reduced cell division, and complete disorganization of the meristematic zone [19,20]. Furthermore, changes in stomatal behavior can contribute to tolerance, as stomata adjust their opening and closing patterns, as well as morphology and cell structure, thereby modulating the absorption and transport of metals [21–23].

Cd accumulation in plant tissues results in damage to the photosynthetic apparatus. At high concentrations, cadmium can compromise the structure of mesophyll cells, leading to disorganization of grana and thylakoid lamellae in chloroplasts, thereby affecting their integrity and reducing chlorophyll content [24]. Furthermore, Cd can replace metal ions, such as Ca^{2+} and Mg^{2+}, within the chlorophyll molecule, affecting its biosynthesis [25,26]. Chlorophyll a (Chl *a*) participates in the capture and conversion of light energy in the central complexes of photosystems I (PSI) and II (PSII). At the same time, Chlorophyll b (Chl *b*) contributes to the capture of light energy in the peripheral light-harvesting complexes of PSI (LHCI) and PSII (LHCII) [27]. Thus, cadmium toxicity causes disturbances to chlorophyll fluorescence, affecting parameters such as the electron transport rate (ETR), the maximum quantum yield of PSII photochemistry (F_v/F_m) [28], the effective quantum yield of PSII photochemistry (Φ_{PSII}), and the photochemical extinction coefficient (q_P) [29]. Therefore, there is a need for a reliable strategy to reduce Cd toxicity and minimize its accumulation in plants, thereby improving plant growth [30].

Brassinosteroids (BRs) are a class of plant hormones belonging to the polyhydroxylated steroid group, mainly involved in various growth and developmental processes [31], such as cell expansion, division, and differentiation [32]. 24-Epibrassinolide (EBR), a plant growth regulator present in plants, regulates growth and development and is widely used to improve plant tolerance to stress [33]. The pathways involved in the stress response include activation of the antioxidant system [34], modulation of root architecture, increased formation and development of lateral roots [35], facilitation of metal sequestration in cell walls, thus reducing their absorption and translocation [36,37], and modulation of gene expression [38].

Several studies have shown that BRs perform multiple physiological and biochemical functions to neutralize the harmful effects caused by abiotic stresses [39–42], especially heavy metal stress, improving the activity of antioxidant enzymes [13,43], altering cell

membrane permeability [44,45], ensuring the homeostasis of essential elements [46,47] and reducing the absorption of these toxic elements [48,49]. Given this, this research hypothesizes that EBR mitigates the adverse effects of Cd stress on soybean plants. Thus, this study aimed to investigate whether the exogenous EBR application can attenuate oxidative damage to the photosynthetic apparatus in soybean plants subjected to cadmium stress and to evaluate the modifications in leaf and root anatomical structures, stomatal variables, biochemical responses related to redox metabolism, and nutritional status.

2. Results

2.1. EBR Minimized Cd Content in Plants Exposed to Excess Cd

Plants subjected to treatment with 500 µM Cd showed increases in Cd content in their tissues (Table 1). However, treatment with EBR (100 nM) promoted a decrease in Cd accumulation in the root, stem, and leaf of 37%, 78%, and 46%, respectively, compared to the Cd treatment in the absence of EBR.

Table 1. Cd contents in soybean plants sprayed with EBR and exposed to Cd excess.

Cd^{2+}	EBR	Cd in Root (µg g DM^{-1})	Cd in Stem (µg g DM^{-1})	Cd in Leaf (µg g DM^{-1})
–	–	0.12 ± 0.01 c	0.04 ± 0.01 c	0.08 ± 0.01 c
–	+	0.13 ± 0.01 c	0.02 ± 0.01 c	0.04 ± 0.01 c
+	–	744.72 ± 16.56 a	14.48 ± 0.24 a	14.38 ± 0.26 a
+	+	472.28 ± 19.05 b	3.20 ± 0.06 b	7.74 ± 0.19 b

Cd^{2+} = Cadmium. Columns with different letters indicate significant differences from the Scott–Knott test ($p < 0.05$). Values described correspond to means from five repetitions and standard deviations.

2.2. Spraying with EBR Provided Protection Against Cd Toxicity in Roots and Leaves

Treatment with 500 µM Cd caused reductions in the values of root epidermis thickness (RET), root endodermis thickness (RDT), root cortex thickness (RCT), vascular cylinder diameter (VCD), and root metaxylem diameter (RMD) of soybean plants (Table 2 and Figure 1). However, plants pre-treated with EBR and subjected to excess Cd showed increases ($p < 0.05$) of 11%, 12%, 18%, and 21% in RDT, RCT, VCD, and RMD, respectively, when compared to the same treatment in the absence of the steroid. In leaf tissues, Cd toxicity caused deleterious effects (Table 2 and Figure 1). However, plants treated with EBR, associated with excess Cd, showed significant increases in epidermis thickness from adaxial leaf side (ETAd), epidermis thickness from abaxial leaf side (ETAb), palisade parenchyma thickness (PPT) and spongy parenchyma thickness (SPT) of 5%, 7%, 11% and 24%, respectively, and a reduction in ratio PPT/SPT of 10%, compared to the treatment with excess Cd alone.

Table 2. Structures of root and leaf in soybean plants sprayed with EBR and exposed to Cd excess.

Cd^{2+}	EBR	RET (µm)	RDT (µm)	RCT (µm)	VCD (µm)	RMD (µm)
–	–	1.26 ± 0.05 b	1.49 ± 0.04 b	22.71 ± 1.88 a	31.31 ± 1.19 b	3.61 ± 0.19 b
–	+	1.44 ± 0.08 a	1.75 ± 0.08 a	24.10 ± 1.13 a	38.50 ± 1.34 a	3.95 ± 0.20 a
+	–	1.05 ± 0.03 d	1.04 ± 0.09 d	19.16 ± 0.60 c	21.76 ± 1.01 d	2.60 ± 0.10 d
+	+	1.13 ± 0.04 c	1.16 ± 0.05 c	21.37 ± 0.48 b	25.59 ± 1.51 c	3.15 ± 0.11 c
Cd^{2+}	**EBR**	**ETAd (µm)**	**ETAb (µm)**	**PPT (µm)**	**SPT (µm)**	**Ratio PPT/SPT**
–	–	16.24 ± 0.49 a	17.74 ± 0.70 a	52.81 ± 2.30 a	127.80 ± 9.69 a	0.42 ± 0.04 b
–	+	16.67 ± 0.37 a	17.98 ± 0.54 a	55.94 ± 1.39 a	132.45 ± 4.00 a	0.42 ± 0.01 b
+	–	14.66± 0.40 c	14.40 ± 0.44 c	46.24 ± 2.13 b	92.44 ± 2.13 c	0.50 ± 0.04 a
+	+	15.34 ± 0.33 b	15.43 ± 0.81 b	51.31 ± 2.85 a	114.59 ± 4.61 b	0.45 ± 0.01 b

RET = Root epidermis thickness; RDT = Root endodermis thickness; RCT = Root cortex thickness; VCD = Vascular cylinder diameter; RMD = Root metaxylem diameter; ETAd = Epidermis thickness from adaxial leaf side; ETAb = Epidermis thickness from abaxial leaf side; PPT = Palisade parenchyma thickness; SPT = Spongy parenchyma thickness. Columns with different letters indicate significant differences from the Scott–Knott test ($p < 0.05$). Values described correspond to means from five repetitions and standard deviations.

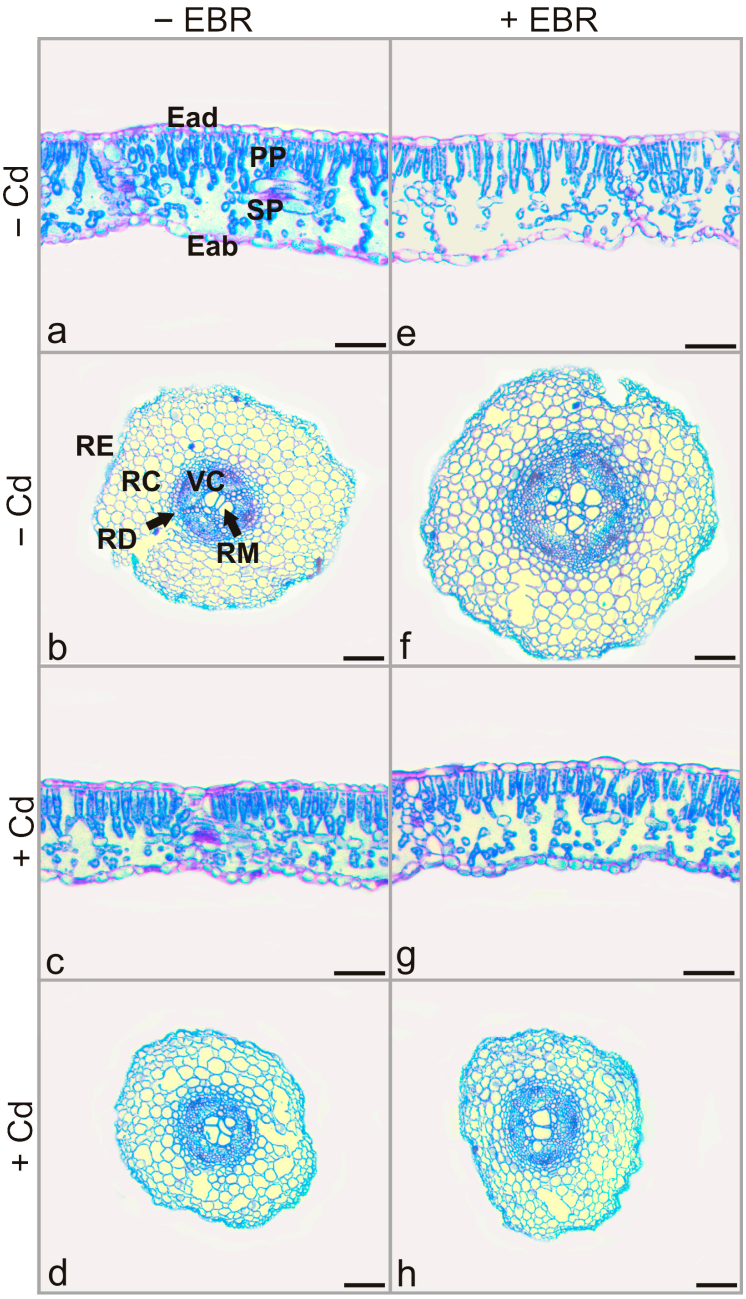


Figure 1. Leaf and root cross sections in soybean plants sprayed with EBR and exposed to Cd excess. $-Cd^{2+}/-$EBR (**a**,**b**), $-Cd^{2+}/+$EBR (**e**,**f**), $+Cd^{2+}/-$EBR (**c**,**d**), $+Cd^{2+}/+$EBR (**g**,**h**). Legends: Ead = adaxial epidermis; Eab = adaxial epidermis; PP = palisade parenchyma; SP = spongy parenchyma; RE = root epidermis; RC = root cortex; RD = root endodermis; VC = vascular cylinder; RM = root metaxylem. Bars (leaf) = 50 µm and bars (root) = 100 µm.

2.3. Steroids Promote Nutritional Balance and Metal Homeostasis

Excess Cd reduced macro- and micronutrient levels in roots, stems, and leaves, whereas EBR spraying increased these levels in the tissues (Table 3). For the roots, the increases obtained by the Cd treatment combined with 100 nM EBR were 10%, 83%, 22%, 13%, 38%, and 15% for potassium (K), calcium (Ca), magnesium (Mg), manganese (Mn), iron (Fe), and zinc (Zn), respectively. The stems showed increases of 18%, 17%, 11%, 39%, 13%, and 27%, respectively, and in the leaves, the increases were 9%, 28%, 20%, 20%, 16%, and 17% for K, Ca, Mg, Mn, Fe, and Zn, in that order, compared to the treatment without EBR.

Table 3. Nutrient contents in soybean plants sprayed with EBR and exposed to Cd excess.

Cd^{2+}	EBR	K (mg g DM^{-1})	Ca (mg g DM^{-1})	Mg (mg g DM^{-1})	Mn (µg g DM^{-1})	Fe (µg g DM^{-1})	Zn (µg g DM^{-1})
				Contents in root			
–	–	32.40 ± 0.80 a	18.02 ± 1.05 b	12.75 ± 0.31 b	505.26 ± 5.87 a	5194.09 ± 63.96 b	29.98 ± 0.56 a
–	+	33.24 ± 0.31 a	19.71 ± 0.89 a	13.94 ± 0.17 a	514.17 ± 18.99 a	5671.43 ± 36.80 a	30.02 ± 0.15 a
+	–	27.90 ± 0.58 c	7.98 ± 0.53 d	9.81 ± 0.40 d	421.71 ± 7.83 c	3256.62 ± 17.05 d	23.66 ± 0.62 c
+	+	30.81 ± 0.80 b	14.59 ± 0.78 c	11.97 ± 0.37 c	476.91 ± 11.50 b	4491.65 ± 88.78 c	27.28 ± 0.91 b
				Contents in stem			
–	–	53.14 ± 0.50 b	8.58 ± 0.50 a	2.91 ± 0.17 a	27.60 ± 0.87 a	93.03 ± 0.32 b	18.17 ± 0.81 a
–	+	54.10 ± 0.78 a	8.77 ± 0.43 a	3.00 ± 0.04 a	28.83 ± 0.30 a	98.38 ± 1.59 a	18.57 ± 0.72 a
+	–	44.20 ± 0.68 c	6.58 ± 0.56 c	2.02 ± 0.07 c	17.91 ± 1.35 c	47.82 ± 2.11 d	13.27 ± 0.39 c
+	+	52.26 ± 0.96 b	7.69 ± 0.43 b	2.25 ± 0.03 b	24.80 ± 0.94 b	53.91 ± 1.02 c	16.88 ± 0.31 b
				Contents in leaf			
–	–	30.44 ± 0.77 a	13.30 ± 0.74 b	5.54 ± 0.42 a	72.28 ± 0.87 a	164.92 ± 4.13 a	34.84 ± 0.42 a
–	+	31.76 ± 1.90 a	14.81 ± 0.94 a	5.64 ± 0.33 a	73.13 ± 1.98 a	170.92 ± 4.99 a	35.85 ± 0.73 a
+	–	26.43 ± 1.10 c	9.55 ± 0.69 d	3.62 ± 0.35 c	56.63 ± 0.95 c	120.36 ± 0.78 c	23.36 ± 0.88 c
+	+	28.81 ± 0.93 b	12.22 ± 0.42 c	4.36 ± 0.27 b	68.03 ± 1.12 b	139.36 ± 6.58 b	27.26 ± 0.92 b

K = potassium; Ca = calcium; Mg = magnesium; Mn = manganese; Fe = iron; Zn = zinc. Columns with different letters indicate significant differences from the Scott–Knott test ($p < 0.05$). Values described correspond to means from five repetitions and standard deviations.

2.4. EBR Positively Modulated Stomatal Performance

Excess Cd caused harmful interference in stomatal structures (Table 4), while steroid spraying in plants exposed to Cd stress promoted improvements in stomatal performance. On the adaxial surface, plants treated with 100 nM EBR + 500 µM Cd obtained significant increases in stomatal density (SD) and stomatal index (SI) of 18% and 80%, respectively, and a reduction in equatorial diameter of the stomata (EDS) of 7%, when compared to the 0 nM EBR + 500 µM Cd treatment. For the abaxial surface, EBR promoted increases of 5% and 32% in SD and SI, respectively, whereas polar diameter of the stomata (PDS) and EDS showed reductions of 5% and 6%, respectively, compared with the equivalent treatments without EBR.

Table 4. Stomatal variables in soybean plants sprayed with EBR and exposed to Cd excess.

Cd^{2+}	EBR	SD (Stomata per mm^2)	PDS (µm)	EDS (µm)	SF	SI
			Adaxial face			
–	–	174.70 ± 8.89 a	21.53 ± 1.70 b	10.84 ± 0.50 c	1.99 ± 0.15 a	10.40 ± 0.84 b
–	+	180.08 ± 10.80 a	20.84 ± 1.77 b	10.14 ± 0.32 c	2.06 ± 0.20 a	11.41 ± 1.07 a
+	–	132.77 ± 7.46 c	23.74 ± 1.90 a	14.20 ± 0.99 a	1.68 ± 0.15 b	4.28 ± 0.34 d
+	+	156.90 ± 7.83 b	22.67 ± 1.28 a	13.16 ± 1.05 b	1.73 ± 0.05 b	7.69 ± 0.68 c
			Abaxial face			
–	–	320.49 ± 11.76 b	23.75 ± 1.15 b	11.39 ± 0.84 c	2.09 ± 0.15 a	17.14 ± 0.80 a
–	+	342.42 ± 10.58 a	23.10 ± 0.81 c	10.92 ± 0.84 c	2.13 ± 0.17 a	17.90 ± 1.19 a
+	–	293.50 ± 19.57 d	25.64 ± 0.75 a	13.62 ± 0.51 a	1.88 ± 0.04 b	9.78 ± 0.86 c
+	+	307.48 ± 6.33 c	24.38 ± 0.57 b	12.75 ± 0.37 b	1.91 ± 0.03 b	12.93 ± 1.00 b

SD = Stomatal density; PDS = Polar diameter of the stomata; EDS = Equatorial diameter of the stomata; SF = Stomatal functionality; SI = Stomatal Index. Columns with different letters indicate significant differences from the Scott–Knott test ($p < 0.05$). Values described correspond to means from five repetitions and standard deviations.

2.5. Pretreatment with EBR Induces Benefits to the Antioxidant System and Reduces ROS Concentration

Cd stress caused significant increases in the activity of the antioxidant enzymes superoxide dismutase (SOD), catalase (CAT), ascorbate peroxidase (APX), and peroxidase (POX) (Figure 2). Spraying 100 nM EBR on plants exposed to Cd^{2+} promoted increases of 25%, 28%, 30% and 48% in SOD, CAT, APX and POX, respectively, when compared to Cd^{2+} treatment without the steroid. Regarding oxidative stress indicators, the production of oxidative compounds was significantly increased in plants exposed to excess Cd (Figure 3). However, pretreatment with 100 nM EBR in plants under Cd stress favored a reduction in

the content of superoxide (O_2^-), hydrogen peroxide (H_2O_2), malondialdehyde (MDA) and electrolyte leakage (EL) compounds of 16%, 8%, 12% and 14%, respectively, compared to the treatment of 0 nM EBR + 500 µM Cd.

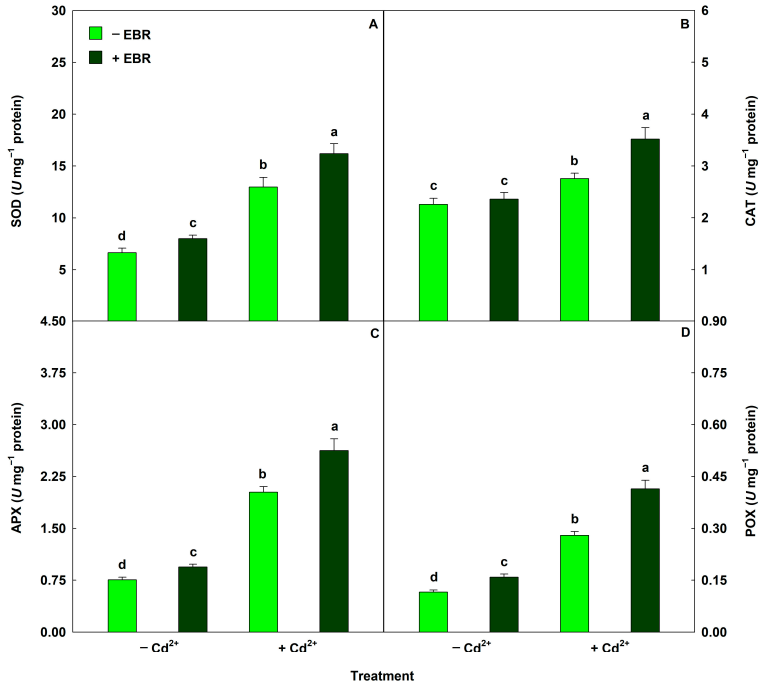


Figure 2. Activities of superoxide dismutase (SOD; (**A**)), catalase (CAT; (**B**)), ascorbate peroxidase (APX; (**C**)) and peroxidase (POX; (**D**)) in soybean plants sprayed with EBR and Cd excess. Columns with different letters indicate significant differences from the Scott–Knott test ($p < 0.05$). Columns correspond to means from five repetitions and standard deviations.

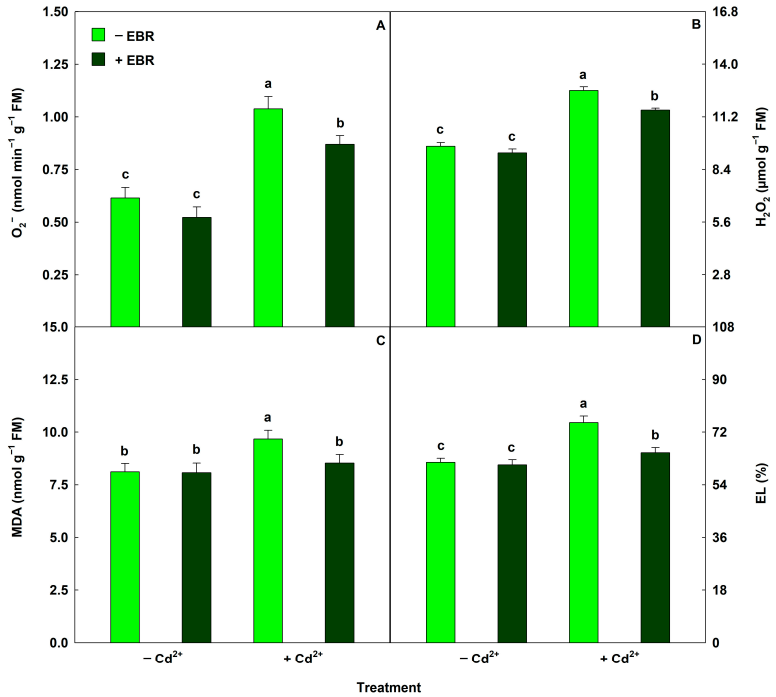


Figure 3. Superoxide (O_2^-; (**A**)), hydrogen peroxide (H_2O_2; (**B**)), malondialdehyde (MDA; (**C**)) and electrolyte leakage (EL; (**D**)) in soybean plants sprayed with EBR and Cd excess. Columns with different letters indicate significant differences from the Scott–Knott test ($p < 0.05$). Columns correspond to means from five repetitions and standard deviations.

2.6. EBR Alleviated the Negative Interferences of Cd on Pigments, Light Capture, and Gas Exchange

Photosynthetic pigments were reduced in plants treated with 500 µM Cd (Table 5). However, the application of 100 nM EBR in plants exposed to Cd toxicity increased ($p < 0.05$) chlorophyll *a* (Chl *a*), chlorophyll *b* (Chl *b*), total chlorophyll (Chl Total), and carotenoids (Car) by 43%, 45%, 44%, and 58%, respectively, compared to the treatment with Cd alone. Regarding light capture, exposure to Cd favored an increase in minimal fluorescence yield of the dark-adapted state (F_0) and a reduction in maximal quantum yield of PSII photochemistry ($F_v/F_{m)}$ (Figure 4). However, plants subjected to Cd exposure associated with 100 nM EBR showed a 7% reduction in F_0 and a 2% increase in F_v/F_m, respectively, compared to the same treatment without EBR. Furthermore, exposure to Cd reduced effective quantum yield of PSII photochemistry (Φ_{PSII}), Photochemical quenching coefficient (qP), and electron transport rate (ETR), and increased relative energy excess at the PSII level (EXC) (Table 5). However, plants treated with 100 nM EBR + 500 µM Cd showed increases of 18%, 11%, and 18% in Φ_{PSII}, q_P, and ETR, respectively, and a decrease of 6% in EXC compared with the treatment with 0 nM EBR + 500 µM Cd. For gas exchange, Cd^{2+} decreased PN, WUE, and P_N/C_i, and increased *E*, g_s, and C_i (Table 5). However, pretreatment with EBR in plants exposed to excess Cd promoted increases in net photosynthetic rate (P_N), water-use efficiency (WUE), and carboxylation instantaneous efficiency (P_N/C_i) of 21%, 64%, and 33%, respectively, and reductions in transpiration rate (*E*), stomatal conductance (g_s), and intercellular CO_2 concentration (C_i) of 26%, 28%, and 9%, respectively, compared to the same treatment in the absence of the steroid.

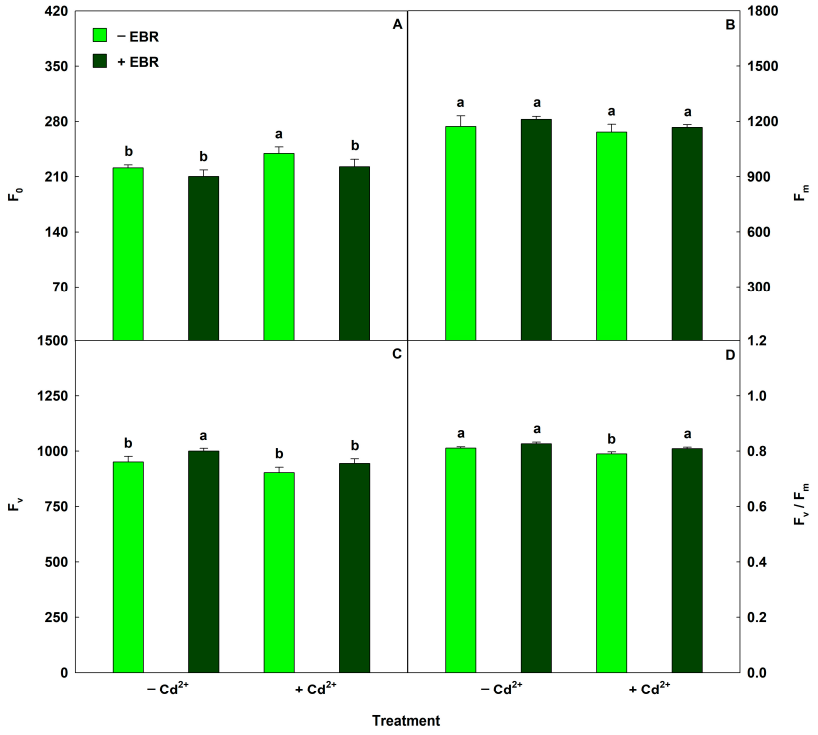


Figure 4. Minimal fluorescence yield of the dark-adapted state (F_0; (**A**)), maximal fluorescence yield of the dark-adapted state (F_m; (**B**)), variable fluorescence (F_v; (**C**)) and maximal quantum yield of PSII photochemistry (F_v/F_m; (**D**)) in soybean plants sprayed with EBR and exposed to Cd excess. Bars with different letters indicate significant differences from the Scott–Knott test ($p < 0.05$). Columns correspond to means from five repetitions and standard deviations.

Table 5. Photosynthetic pigments, chlorophyll fluorescence and gas exchange in soybean plants sprayed with EBR and exposed to Cd excess.

Cd^{2+}	EBR	Chl *a* (mg g^{-1} FM)	Chl *b* (mg g^{-1} FM)	Total Chl (mg g^{-1} FM)	Car (mg g^{-1} FM)	Ratio Chl *a*/Chl *b*	Ratio Total Chl/Car
–	–	12.23 ± 0.60 a	3.16 ± 0.23 a	15.39 ± 0.58 a	1.08 ± 0.02 b	3.89 ± 0.37 a	14.31 ± 0.74 a
–	+	12.62 ± 0.66 a	3.29 ± 0.20 a	15.91 ± 0.81 a	1.12 ± 0.03 a	3.84 ± 0.16 a	14.20 ± 0.78 a
+	–	6.33 ± 0.06 c	1.54 ± 0.13 c	7.87 ± 0.17 c	0.50 ± 0.03 d	4.12 ± 0.35 a	15.90 ± 1.10 a
+	+	9.07 ± 0.59 b	2.24 ± 0.17 b	11.31 ± 0.68 b	0.79 ± 0.04 c	4.07 ± 0.33 a	14.42 ± 1.38 a
Cd^{2+}	EBR	Φ_{PSII}	q_P	NPQ	ETR (µmol m^{-2} s^{-1})	EXC (µmol m^{-2} s^{-1})	ETR/P_N
–	–	0.471 ± 0.027 a	0.443 ± 0.027 a	0.56 ± 0.04 b	69.19 ± 3.98 a	0.420 ± 0.032 c	3.77 ± 0.10 a
–	+	0.481 ± 0.026 a	0.470 ± 0.027 a	0.54 ± 0.04 b	70.69 ± 3.85 a	0.418 ± 0.030 c	3.76 ± 0.11 a
+	–	0.313 ± 0.018 c	0.364 ± 0.028 c	0.67 ± 0.02 a	46.06 ± 2.68 c	0.604 ± 0.021 a	3.21 ± 0.17 b
+	+	0.370 ± 0.025 b	0.404 ± 0.024 b	0.63 ± 0.04 a	54.38 ± 3.73 b	0.543 ± 0.035 b	3.14 ± 0.09 b
Cd^{2+}	EBR	P_N (µmol m^{-2} s^{-1})	*E* (mmol m^{-2} s^{-1})	g_s (mol m^{-2} s^{-1})	C_i (µmol mol^{-1})	WUE (µmol $mmol^{-1}$)	P_N/C_i (µmol m^{-2} s^{-1} Pa^{-1})
–	–	18.34 ± 0.60 a	1.56 ± 0.09 b	0.222 ± 0.019 b	235 ± 14 b	11.80 ± 0.36 b	0.078 ± 0.007 b
–	+	18.78 ± 0.61 a	1.47 ± 0.07 b	0.198 ± 0.013 c	178 ± 13 c	12.83 ± 0.92 a	0.106 ± 0.011 a
+	–	14.35 ± 0.30 c	2.18 ± 0.11 a	0.318 ± 0.015 a	263 ± 12 a	6.61 ± 0.30 d	0.055 ± 0.003 c
+	+	17.33 ± 0.78 b	1.60 ± 0.08 b	0.228 ± 0.024 b	240 ± 19 b	10.82 ± 0.36 c	0.073 ± 0.005 b

Chl *a* = Chlorophyll *a*; Chl *b* = Chlorophyll *b*; Total chl = Total chlorophyll; Car = Carotenoids; Φ_{PSII} = Effective quantum yield of PSII photochemistry; q_P = Photochemical quenching coefficient; NPQ = Nonphotochemical quenching; ETR = Electron transport rate; EXC = Relative energy excess at the PSII level; ETR/P_N = Ratio between the electron transport rate and net photosynthetic rate; P_N = Net photosynthetic rate; *E* = Transpiration rate; g_s = Stomatal conductance; C_i = Intercellular CO_2 concentration; WUE = Water-use efficiency; P_N/C_i = Carboxylation instantaneous efficiency. Columns with different letters indicate significant differences from the Scott–Knott test ($p < 0.05$). Values described correspond to means from five repetitions and standard deviations.

2.7. EBR Mitigates Damage Caused by Excess Cd in Biomass

Plants exposed to treatment with 500 µM Cd showed significant reductions in biomass (Figures 5 and 6). However, spraying with EBR promoted increases ($p < 0.05$) in leaf dry matter (LDM), root dry matter (RDM), stem dry matter (SDM), and total dry matter (TDM) of 175%, 163%, 170%, and 172%, respectively, when compared to the same treatment in the absence of the steroid.

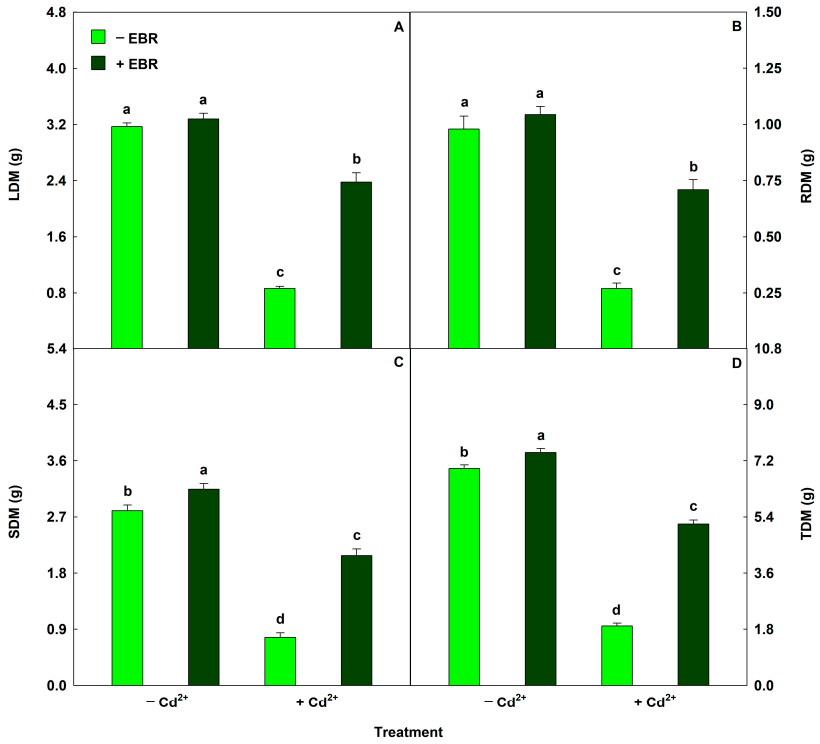


Figure 5. Leaf dry matter (LDM; (**A**)), root dry matter (RDM; (**B**)), stem dry matter (SDM; (**C**)) and total dry matter (TDM; (**D**)) in soybean plants sprayed with EBR and Cd excess. Columns with different letters indicate significant differences from the Scott–Knott test ($p < 0.05$). Columns correspond to means from five repetitions and standard deviations.

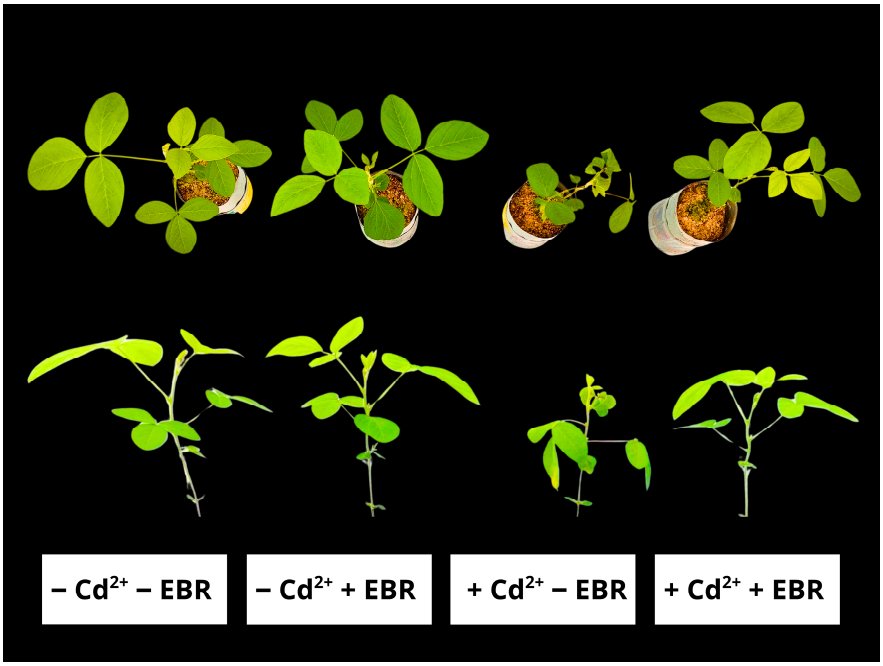


Figure 6. Upper and side views of soybean plants sprayed with EBR and Cd excess.

3. Discussion

This research confirms the steroid's role in mitigating the harmful effects of heavy metals, more specifically improving anatomical structures and the antioxidant defense system (Figure 7).

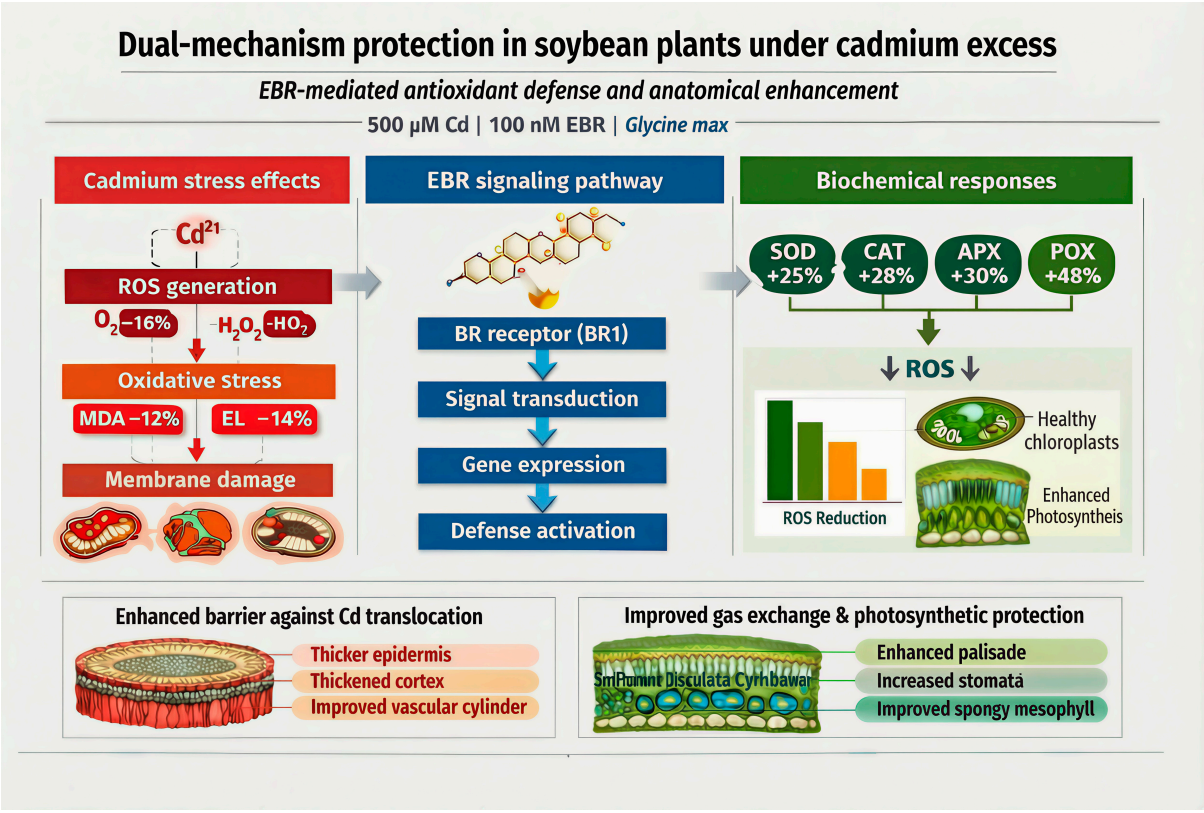


Figure 7. Mechanism protection in soybean plants sprayed with EBR and Cd excess. Created with Manus AI according to the terms and conditions of the subscription.

Cd content found in the roots, stem, and leaves of soybean plants showed significant increases induced by the exogenous application of 500 μM Cd. On the other hand, treatment with 100 nM EBR reduced Cd levels. These results may be related to EBR's ability to promote changes in root cell walls, increasing their binding capacity for Cd ions and controlling their entry [48]. Furthermore, in higher plants, application of EBR stimulates biosynthesis of phytochelatins, which can reduce metal toxicity [16,50]. Foliar application of EBR reduced Cd concentration in wheat roots (39%), shoots (46%), and grains (27%) under elevated CO_2 conditions [51]. Similarly, supplementation with EBR in Cd-stressed pea seedlings reduced Cd accumulation in roots, shoots, and leaves by 38%, 28%, and 48%, respectively [52].

EBR alleviated the damage caused by Cd and increased the absorption of macronutrients (K, Ca, and Mg) and micronutrients (Mn, Fe, and Zn). These results may be related to improvements obtained in root structures (RDT, RCT, VCD, and RMD), which favored nutrient absorption. The observed improvement in root structure thickness is associated with EBR's promotion of cell elongation and division [53]. Furthermore, the steroid plays a regulatory role in cell membrane permeability, strengthening root activity and improving the efficiency of water and nutrient absorption [54]. Concomitantly, the increase in RMD suggests wider xylem vessels, which maximizes the space for vascular bundles, enhancing hydraulic transport and ionic absorption [55], corroborated by increases in the accumulation of macronutrients (K, Ca, and Mg) and micronutrients (Mn, Fe, and Zn). Improvements in root structure were observed in tomato plants exposed to salinity after foliar application of 100 nM EBR, with increases of 12%, 10%, 9%, 66%, and 119% in RET, RDT, RCD, VCD, and RMD, respectively [56]. EBR pretreatment promoted increases in K^+, Ca^{2+}, and Mg^{2+} levels by 68%, 58%, and 81%, respectively, under 100 mM NaCl, and by 41%, 72%, and 70%, respectively, under 200 mM NaCl conditions [57].

Spraying EBR on plants exposed to excess Cd promoted changes in leaf anatomical structures. The increases observed in ETad, ETab, PPT, and SPT indicate that the steroid stimulated leaf protection and gas exchange efficiency. These effects on ETad and ETab are related to the benefits promoted by EBR for leaf growth [58], acting on cell division and expansion [59], membrane stabilization [60], and protection and adaptation of the mesophyll and epidermis, maximizing water-use efficiency [61], as corroborated by the increase in WUE obtained in this study. The increase in mesophyll thickness enhances light absorption and CO_2 fixation [62]. Thus, the increases in PPT and SPT demonstrate the improvement in gas exchange promoted by EBR, as evidenced by the superior performance in P_N and P_N/C_i observed in this research. Conditioning with EBR in sorghum genotypes, both sensitive and tolerant to salinity, promoted anatomical adaptations in leaves, including the restoration of mesophyll cells [63]. Additionally, increases in ETad, ETab, PPT, and SPT were observed in tomato plants under both low and high Zn levels after EBR application [64].

EBR positively modulated stomatal characteristics (SD, SI, PDS, and EDS), mitigating the toxic effects caused by excess Cd. This effect stems from the steroid's ability to coordinate stomatal performance by regulating the expression of genes crucial for its development, such as *SPCH*, *BIN2* [65], *BZR1*, *BES1*, *MKK9*, and *FAMA* [66], modulating stomatal function and gas exchange [67], notably by increasing CO_2 influx [68], as evidenced by the increases in PPT, SPT, P_N, and P_N/C_i identified in this study. Modifications in stomatal shape are directly associated with stomatal size and functionality [69], serving as essential indicators of the efficiency of CO_2 diffusion to the carboxylation sites and transpiration [70,71]. In tomato plants subjected to Pb stress, EBR application, alone or combined with DOP, promoted increases in SD (68%), SF (8%), and SI (40%), and reductions in PDS (24%) and EDS (30%) on the adaxial face, while on the abaxial face increases of 76%, 4%, and 45% were

observed in SD, SF, and SI, respectively, along with reductions of 14% and 18% in PDS and EDS [72]. Similarly, in soybean plants subjected to acid rain stress, EBR (100 nM) induced increases in SD, EDS and SI and reductions in PDS and EDS [73].

Plants treated with 100 nM EBR + 500 µM Cd showed increases in the activity of the antioxidant defense system. The increases observed in the activity of the enzymes SOD, CAT, APX, and POX can be considered a ROS-dependent response [74], since the overaccumulation of ROS activates the transcription of stress-responsive genes, including those encoding antioxidant enzymes, such as the gene encoding BSK 1 (BR 1 signaling kinase), which is positively regulated to attenuate oxidative stress, mitigating the damage caused by cadmium [75,76]. EBR application improved Pb-induced oxidative stress in fenugreek plants by enhancing the antioxidant defense system and positively regulating the expression of SOD and CAT genes [77]. Similar to our results, increases in SOD (50%), CAT (27%), APX (40%), and POX (19%) activities were observed in soybean plants under Ni stress following exogenous EBR application [78].

Plants exposed to excess Cd showed increased levels of oxidative compounds, but EBR spraying attenuated the harmful interference, reducing the levels of O_2^-, H_2O_2, MDA, and EL. Excessive accumulation of ROS triggers lipid peroxidation and can damage cell membrane integrity, negatively modulating cellular function [79]. While the steroid reduces oxidative stress by binding ROS to membrane proteins, it also restricts the absorption of heavy metals by stabilizing the electrical properties and enzymatic activities of cell membranes [80]. Exogenous EBR supply improved membrane stability in soybean seedlings under Cr stress by reducing MDA (40.9%), O_2^- (45%), H_2O_2 (38%), and EL (32%) levels [81]. Under Zn stress in watermelon seedlings, EBR alleviated oxidative damage, as evidenced by reductions in H_2O_2 and MDA levels [82].

Treatment with 500 µM Cd significantly reduced chloroplast pigments. Cd toxicity disrupts the photosynthetic apparatus by inhibiting chlorophyll synthesis, reducing chlorophyll synthase activity, damaging chloroplast structures, reducing stomatal opening, and lowering chlorophyll content and photosynthesis [83]. However, plants treated with EBR showed increases in Chl *a*, Chl *b*, total Chl, and Car, due to the steroid's contribution to maintaining the stability of chlorophyll by favoring synthesis and reducing degradation of the molecule (inhibiting chlorophyllase activity), as well as protecting the structural integrity of chloroplasts, mitigating membrane damage [84], validated by the reduction in MDA and EL. Increases in Chl *a*, Chl *b*, Car, and total Chl levels were observed following EBR application, contributing to the attenuation of Cd stress in peanut seedlings [85]. Similarly, EBR application in maize plants under 50 mg Cd kg^{-1} soil resulted in increases of 17%, 34%, 18%, and 15% in Chl *a*, Chl *b*, total Chl, and carotenoid content, respectively [86].

Plants exposed to excess Cd showed an increase in F_0 and a reduction in F_v/F_m. Changes in F_0 depend on factors that occur during energy dissipation, such as damage or inactivation of PSII, which can increase F_0 [87,88]. The decrease in F_v/F_m in plants indicates a specific phenomenon of photodamage to the PSII reaction centers under stress [89]. However, the application of EBR attenuated the deleterious effects on chlorophyll fluorescence. The observed increase in F_v/F_m and reduction in F_0 suggest that the steroid benefits the PSII reaction center, increasing the efficiency of photon capture and conversion. EBR reduces the intensity of photoinhibition in plants, preventing damage to the PSII reaction center and increasing the capacity for excitation energy transfer from the antenna to PSII, thereby improving the performance of the photosynthetic machinery [90]. EBR supplementation increased F_v/F_m in maize seedlings under Al stress, indicating improvements in chlorophyll fluorescence and photosynthetic performance [91]. Corroborating our results, EBR pretreatment in soybean plants under Fe-deficient conditions reduced F_0 by 16% and increased F_v/F_m by 6% [92].

EBR alleviated the negative interferences induced by Cd in chlorophyll fluorescence. Cd^{2+} can affect all electron transport in PSII: inhibiting the oxygen-evolving complex (OEC), blocking electron transport between Q_A and Q_B [93], and disrupting Q_B function or altering the Q_B reduction electron transport pathway [94]. However, EBR promoted increases in Φ_{PSII}, q_p, and ETR due to the role of this steroid in increasing the proportion of open PSII reaction centers and the oxidation state of Q_A, improving PSII reaction center activity and increasing the efficiency of radiation energy transfer and conversion [95]. Furthermore, EBR regulates transcripts encoding PSII OEC proteins, PS I subunit, light-harvesting chlorophyll protein complexes I and II, and ferredoxin [96]. Additionally, EBR reduced the EXC value, confirming the steroid's role in maintaining the stability of the electron transport chain and PSII activity, and in increasing the density of active reaction centers, alleviating photoinhibition and enhancing heat dissipation in PSII antennas [97]. Increases in Φ_{PSII} and q_P, as well as reductions in NPQ, were observed in *Brassica juncea* plants under cadmium toxicity supplemented with EBR [98]. EBR application in grape plants under Cd stress improved F_v/F_m, Φ_{PSII} and q_P values, while reducing NPQ [99].

EBR mitigated the deleterious effects of 500 µM Cd on gas exchange. Increases in P_N, WUE, and P_N/C_i obtained with EBR pretreatment are related to the steroid-stimulated improvements in Φ_{PSII}, q_P, and ETR values verified in this research, demonstrating the effectiveness of EBR in increasing photosynthesis, particularly in increasing the activation state of RuBisCO, an essential contributor to the photosynthetic carbon reduction cycle [100]. It is widely recognized that plants close their stomata to avoid excessive water loss, resulting in reduced g_s, consequently, there is a decrease in E and C_i [101]. Therefore, the reductions obtained in E, g_s, and C_i may be related to a protective measure induced by EBR, since the decrease in these parameters did not affect the net photosynthetic rate, verified by the increase in P_N, WUE, and P_N/C_i, which the increases in SD and SI, and reductions in PDS and EDS can corroborate. Increases in P_N, g_s, and E were observed in melon plants at 15 + 30 days after transplant (DAT) following different EBR application frequencies (0, 15, 30, and 45 DAT) [102]. Similar to our results, 100 nM EBR pretreatment in soybean plants under different B levels (low, control, and high) promoted increases in P_N, WUE and P_N/C_i, and reductions in C_i, E and g_s under control and high B conditions (30 and 1500 µM B) [103].

Cd-induced stress considerably reduced the biomass of roots, stems, and leaves of soybean plants, resulting in decreased growth. This reduction is associated with disturbances caused by the metal in nutrient absorption, plant metabolism, water relations, gas exchange, photosynthetic efficiency, and cell membrane integrity [104,105]. In contrast, EBR promoted increases in LDM, SDM, RDM, and TDM; these results are strongly associated with the integrated functions of the steroid in modulating the antioxidant system, regulating nutritional status, gas exchange, stabilizing chloroplast pigments, photochemical efficiency, and anatomical adaptations [63,106,107]. Corroborating our results, improvements in the dry biomass of roots and shoots of soybean plants promoted by EBR were reported in a study evaluating the potential of the simple and combined application of titanium oxide nanoparticles and EBR in alleviating Cd toxicity [108]. Similarly, EBR application (0.1 µM) promoted increases in root and shoot biomass accumulation in rice plants exposed to Cd stress [36].

4. Materials and Methods

4.1. Location and Growth Conditions

Universidade Federal Rural da Amazônia, Paragominas, Brazil (2°55′ S, 47°34′ W), hosted the experiment. Controlled temperature and humidity were used in the greenhouse

investigation. Minimum, maximum, and median temperatures were 25.3, 30.9, and 26.8 °C. In the experiment, relative humidity ranged from 60% to 80%.

4.2. Plants, Containers and Acclimation

Seeds of *Glycine max* (L.) Merr. var. M8644RR Monsoy™ were germinated and grown in 1.2 L pots [109]. This plant material has been widely used by farmers in this region agricultural for over 10 years and has broad adaptability. The nutritive solution used for plant nutrition initially had 50% ionic strength (4th day) and later modified to 100% after two days (6th day), remaining at full ionic strength thereafter [110].

4.3. Experimental Design

Four randomized treatments were used in the experiment: two with cadmium (0 and 500 µM Cd, −Cd and +Cd, respectively) and two with 24-epibrassinolide (0 and 100 nM EBR, −EBR and +EBR, respectively). Each of the four treatments included five replicates, providing 20 experimental units with one plant each.

4.4. 24-Epibrassinolide (EBR) Preparation and Application

12-day-old plants were sprayed with 24-epibrassinolide or Milli-Q water (having the same amount of ethanol as the EBR solution) every five days (12, 17, 22, and 27th day) until day 27. Dissolving the solute in ethanol and diluting with Milli-Q water (1:10,000) yielded EBR (0 and 100 nM, Sigma–Aldrich, Saint Louis, MO, USA) solutions [111].

4.5. Plant Nutrition and Cd Excess

Nutrition solution provided the following macro- and micronutrients to plants [110]. To replicate Cd^{2+} exposure, cadmium chloride ($CdCl_2$) was employed at 0 and 500 µM Cd concentrations [112]. The Cd excess was applied over 10 days (20–30 days post-start) with a 5-day gap between applications. The nutrition solutions were replaced at 07:00 h every three days and pH adjusted to 6.5 with HCl or NaOH. On experiment day 30, all plants' physiological and morphological characteristics were assessed, and leaf tissues were harvested for nutritional, anatomical, and biochemical investigations.

4.6. Determining of Cd and Nutrients

Milled root, stem, and leaf tissues (100 mg) were pre-digested in 50 mL conical tubes with 2 mL subboiled HNO_3. According to [113], 8 mL of a solution comprising 4 mL of H_2O_2 (30% *v*/*v*) and 4 mL of ultra-pure water was put to a Teflon digesting vessel. An inductively coupled plasma mass spectrometer (ICP-MS 7900, Agilent, Santa Clara, CA, USA) measured Cd, K, Ca, Mg, Mn, Fe, and Zn.

4.7. Measurement of Chlorophyll Fluorescence and Gas Exchange

A modulated chlorophyll fluorometer (model OS5p, Opti-Sciences, Hudson, NH, USA) was calibrated [114] to detect fluorescence in fully inflated leaves under light. Gas exchange was measured in the middle region of plants using an infrared gas analyzer (LCPro$^+$, ADC BioScientific, Hoddesdon, Borough of Broxbourne, UK) in a chamber at constant CO_2, photosynthesis, air-flow rate, and temperature (360 µmol mol^{-1} CO_2, 800 µmol photons m^{-2} s^{-1}, 300 µmol s^{-1}, and 28 °C) between 10:00 and 12:00 h. WUE was estimated as P_N divided by E.

4.8. Anatomical Measurements

Samples were taken from the middle leaf blades of fully developed third-node leaves and from roots 5 cm from the root apex. All botanical material was then submerged in 70% (*v*/*v*) fixation solution (formaldehyde at 37%, acetic acid at 70% in proportions of 0.5, 0.5,

and 9.0) for 24 h, dried in ethanol, and embedded in historesin LeicaTM (Leica, Nussloch, Germany). Using a rotating microtome (model Leica RM 2245, Leica Biosystems, Nussloch, Rhein-Neckar-Kreis, Germany), 5 µm transverse slices were produced and stained with toluidine blue [115]. Epidermal impressions were used for stomatal characterization [116]. An optical microscope (Motic BA 310, Motic Group Co., Ltd., Universal, CA, USA) and digital camera (Model Motic 2500) were used to photograph the slides. The photos were analyzed using a Moticplus 2.0 calibrated with a manufacturer micrometer slide.

4.9. Enzymatic Assays and Superoxide

Extraction was performed using 500 mg plant material homogenized with 5 mL of extraction buffer [50 mM phosphate buffer (pH 7.6), 1.0 mM ascorbate and 1.0 mM EDTA] and subsequently centrifuged at 14,000× *g* for 4 min at 3 °C. Finally, the supernatant was collected [117]. In determinations, SOD activity was measured with 0.2 mL supernatant and 2.8 mL reaction mixture [50 mM phosphate buffer (pH 7.6), 0.1 mM EDTA, 13 mM methionine (pH 7.6), 75 µM NBT and 4 µM riboflavin], expressed in units of mg^{-1} protein [118]. CAT activity was evaluated using 0.2 mL of supernatant and 1.8 mL of reaction mixture [50 mM phosphate buffer (pH 7.0) and 12.5 mM hydrogen peroxide], presented in µmol H_2O_2 mg^{-1} protein min^{-1} [119]. APX activity was determined with 0.2 mL of supernatant and 1.8 mL of reaction mixture [50 mM phosphate buffer (pH 7.0), 0.5 mM ascorbate, 0.1 mM EDTA and 1.0 mM hydrogen peroxide], expressed in µmol AsA mg^{-1} protein min^{-1} [120]. POX activity was measured using 0.2 mL of supernatant and 1.78 mL of a reaction mixture [50 mM phosphate buffer (pH 7.0) and 0.05% guaiacol and 20 µL of 10 mM hydrogen peroxide] presented in µmol tetraguaiacol mg^{-1} protein min^{-1} [121]. O_2^- was determined using 1 mL of supernatant extracted above and incubated with a reaction mixture [30 mM phosphate buffer (pH 7.60), 0.51 mM hydroxylamine hydrochloride, 17 mM sulfanilamide, 7 mM α-naphthylamine and ethyl ether] [122]. Total soluble proteins were analyzed according to the Bradford method [123].

4.10. Oxidative Stress Indicators, Chloroplastic Pigments and Biomass

To extract oxidative stress indicators, combine 500 mg of fresh material with 5 mL of 5% (*w*/*v*) trichloroacetic acid. Centrifuge at 15,000× *g* for 15 min at 3 °C to obtain the supernatant [124]. With 0.2 mL of supernatant and 1.8 mL of reaction mixture (2.5 mM potassium phosphate buffer [pH 7.0] and 500 mM potassium iodide), H_2O_2 was measured [125]. MDA was quantified using 0.5 mL of supernatant and 1 mL of reaction mixture (0.5% (*w*/*v*) thiobarbituric acid in 20% trichloroacetic acid) [126]. EL was determined according to the method described in [127]. With 40 mg of leaf tissue homogenized in 8 mL of 90% methanol, photosynthetic pigments Chl *a*, Chl *b*, Car, and total Chl were extracted [128]. Root, stem, and leaf biomass were determined by constant dry weights (g) after drying in a forced-air ventilation oven at 65 °C.

4.11. Data Analysis

The Shapiro–Wilk test confirmed residue normality. The Scott–Knott test at 5% was used to evaluate significant mean differences after one-way ANOVA [129]. Standard deviations were determined for each treatment. Statistical analysis was conducted using R™ software version 4.4.1 [130].

5. Conclusions

EBR mitigated the deleterious effects caused by excess Cd, as evidenced by improvements in anatomical structures (root and leaf) and the antioxidant defense system. This steroid modulated leaf anatomy, increasing the thickness of palisade and spongy parenchyma. In roots, EBR induced protective anatomical adaptations, reflected by in-

creases in the thickness of the endodermis and cortex, and in the diameter of the vascular cylinder and metaxylem, reinforcing root protection, minimizing Cd translocation to the shoot, and, consequently, increasing stress tolerance. Simultaneously, EBR stimulated redox metabolism by increasing the activities of antioxidant enzymes, more specifically superoxide dismutase, catalase, ascorbate peroxidase, and peroxidase. Therefore, EBR reduced the levels of reactive oxygen species, as detected by minor concentrations of superoxide, hydrogen peroxide, malondialdehyde and electrolyte leakage, resulting in less oxidative damage to the photosynthetic apparatus. These results were corroborated by the adaptations observed in stomatal structures, chloroplast pigments, carbon fixation, and chlorophyll fluorescence. Therefore, the results suggest that exogenous EBR treatment attenuates the negative interference induced by Cd excess in soybean plants. Additionally, further research using molecular approaches is necessary to determine genes involved in this tolerance mechanism.

Author Contributions: A.K.d.S.L. served as the advisor for this project, planned all phases of the research, and critically revised the manuscript. A.S.C. conducted the experiment, performed physiological, biochemical, and morphological determinations; they wrote and edited the manuscript. while I.B.V. performed anatomical determinations. C.C.A. and B.L.B. nutritional analysis. All authors have read and agreed to the published version of the manuscript.

Funding: This research had financial supports from Fundação Amazônia de Amparo a Estudos e Pesquisas (FAPESPA/Brazil), Conselho Nacional de Desenvolvimento Científico e Tecnológico (CNPq/Brazil) and Universidade Federal Rural da Amazônia (UFRA/Brazil) to AKSL.

Institutional Review Board Statement: Not applicable.

Informed Consent Statement: Not applicable.

Data Availability Statement: The raw data supporting the conclusions of this article will be made available by the authors on request.

Acknowledgments: ASC was supported with a scholarship from Coordenação de Aperfeiçoamento de Pessoal de Nível Superior (CAPES/Brazil).

Conflicts of Interest: The authors declare no conflicts of interest.

Abbreviations

The following abbreviations are used in this manuscript:

APX	Ascorbate peroxidase
Ca	Calcium
CAR	Carotenoids
CAT	Catalase
Cd	Cadmium
$CdCl_2$	Cadmium chloride
Chl *a*	Chlorophyll a
Chl *b*	Chlorophyll b
C_i	Intercellular CO_2 concentration
CO_2	Carbon dioxide
E	Transpiration rate
EBR	24-epibrassinolide
EDS	Equatorial diameter of the stomata
EL	Electrolyte leakage
ETAb	Epidermis thickness from abaxial leaf side
ETAd	Epidermis thickness from adaxial leaf side
ETR	Electron transport rate

ETR/P_N	Ratio between the apparent electron transport rate and net photosynthetic rate
EXC	Relative energy excess at the PSII level
F_0	Minimal fluorescence yield of the dark-adapted state
Fe	Iron
F_m	Maximal fluorescence yield of the dark-adapted state
F_v	Variable fluorescence
F_v/F_m	Maximal quantum yield of PSII photochemistry
g_s	Stomatal conductance
HMs	Heavy metals
H_2O_2	Hydrogen peroxide
K	Potassium
LDM	Leaf dry matter
MDA	Malondialdehyde
Mg	Magnesium
Mn	Manganese
NPQ	Nonphotochemical quenching
O_2^-	Superoxide
PDS	Polar diameter of the stomata
P_N	Net photosynthetic rate
P_N/C_i	Instantaneous carboxylation efficiency
POX	Peroxidase
PPT	Palisade parenchyma thickness
PSII	Photosystem II
q_P	Photochemical quenching
RCT	Root cortex thickness
RET	Root epidermis thickness
RDM	Root dry matter
RDT	Root endodermis thickness
RMD	Root metaxylem diameter
ROS	Reactive oxygen species
SD	Stomatal density
SDM	Stem dry matter
SF	Stomatal functionality
SI	Stomatal Index
SOD	Superoxide dismutase
SPT	Spongy parenchyma thickness
TDM	Total dry matter
Total Chl	Total Chlorophyll
VCD	Vascular cylinder diameter
WUE	Water-use efficiency
Zn	Zinc
Φ_{PSII}	Effective quantum yield of PSII photochemistry

References

1. He, J.; Chen, Y.; Zhang, M.; Qiu, Y.; Zhou, H.; Li, M. Current Perspectives on Improving Soybean Performance on Saline-Alkaline Lands. *New Crop.* **2025**, *3*, 100079. [CrossRef]
2. Yuan, M.; Wang, T.; Yao, S.; Han, D.; Meng, Y.; Yu, S.; Lu, W. Frequency—Dependent Maize Rotation Modulates Fungal Functions for Sustainable Soybean Production. *Chem. Biol. Technol. Agric.* **2025**, *12*, 144. [CrossRef]
3. Siamabele, B. The Significance of Soybean Production in the Face of Changing Climates in Africa the Significance of Soybean Production in the Face of Changing Climates in Africa. *Cogent Food Agric.* **2021**, *7*, 1933745. [CrossRef]
4. Voora, V.; Bermudez, S.; Le, H.; Larrea, C.; Luna, E. *Soybean Prices and Sustainability*; Global Marketing Report; IISD: Winnipeg MB, Canada, 2024.
5. Persistence, M.R. Soybean By-Products Market. Available online: https://www.persistencemarketresearch.com/market-research/soybean-by-products-market.asp (accessed on 12 February 2026).

6. Fraanje, W.; Garnett, T. Soy: Food, Feed, and Land Use Change. *Food Clim. Res. Netw.* **2020**, *44*, 31–34.
7. Alhaj Hamoud, Y.; Shaghaleh, H.; Zia-ur-Rehman, M.; Rizwan, M.; Umair, M.; Usman, M.; Ayub, M.A.; Riaz, U.; Alnusairi, G.S.H.; Alghanem, S.M.S. Cadmium and Lead Accumulation in Important Food Crops Due to Wastewater Irrigation: Pollution Index and Health Risks Assessment. *Heliyon* **2024**, *10*, e24712. [CrossRef]
8. Irshad, M.K.; Zhu, S.; Javed, W.; Cheol, J.; Mahmood, A.; Soo, S.; Jianying, S.; Albasher, G.; Ali, A. Risk Assessment of Toxic and Hazardous Metals in Paddy Agroecosystem by Biochar-for Bio-Membrane Applications. *Chemosphere* **2023**, *340*, 139719. [CrossRef]
9. Haider, F.U.; Liqun, C.; Coulter, J.A.; Cheema, S.A.; Wu, J.; Zhang, R.; Wenjun, M.; Farooq, M. Cadmium Toxicity in Plants: Impacts and Remediation Strategies. *Ecotoxicol. Environ. Saf.* **2021**, *211*, 111887. [CrossRef]
10. Irshad, M.K.; Waseem, M.; Saleem, S.; Ansari, J.R.; Ashraf, S.; Javed, W.; Noman, A.; Aqeel, M.; Rizwan, M.; Mohammed, A.E.; et al. Synergistic Effects of Biochar and Silicon Dioxide Nanoparticles Abate Cadmium Uptake and Oxidative Stress in Tomato: Achieving Crop Resilience and Environmental Sustainability. *Plant Sci.* **2025**, *362*, 112821. [CrossRef] [PubMed]
11. Emamverdian, A.; Ding, Y.; Barker, J.; Liu, G.; Hasanuzzaman, M.; Li, Y.; Ramakrishnan, M.; Mokhberdoran, F. Co-Application of 24-Epibrassinolide and Titanium Oxide Nanoparticles Promotes Pleioblastus Pygmaeus Plant Tolerance to Cu and Cd Toxicity by Increasing Antioxidant Activity and Photosynthetic Capacity and Reducing Heavy Metal Accumulation and Translocati. *Antioxidants* **2022**, *11*, 451. [CrossRef] [PubMed]
12. Farooq, M.; Ullah, A.; Usman, M.; Siddique, K.H.M. Application of Zinc and Biochar Help to Mitigate Cadmium Stress in Bread Wheat Raised from Seeds with High Intrinsic Zinc. *Chemosphere* **2020**, *260*, 127652. [CrossRef] [PubMed]
13. Piacentini, D.; Bellini, C.; Peduzzi, A.; Casentini, B.; Tiraboschi, C.; Cacciotti, A. Arsenite and Arsenate Stress Differently Affect Auxin Distribution in Rice Roots and Brassinosteroids Restore It Sustaining Root System Plasticity. *Plant Stress* **2024**, *11*, 100418. [CrossRef]
14. Shi, J.; Zhou, Y.; Yang, S.; Xue, Y.; Wang, Y.; Hu, H.; Liu, Y. The Key Metabolic Pathway of Roots and Leaves Responses in Arachis Hypogaea under Al Toxicity Stress. *BMC Plant Biol.* **2025**, *25*, 439. [CrossRef]
15. Ali, I.; Hussain, J.; Yanwisetpakdee, B.; Iqbal, I.; Chen, X. The Effects of Monoculture and Intercropping on Photosynthesis Performance Correlated with Growth of Garlic and Perennial Ryegrass Response to Different Heavy Metals. *BMC Plant Biol.* **2024**, *24*, 659. [CrossRef] [PubMed]
16. Guedes, F.R.C.M.; Maia, C.F.; Silva, B.R.S.d.; Batista, B.L.; Alyemeni, M.N.; Ahmad, P.; Lobato, A.K.d.S. Exogenous 24-Epibrassinolide Stimulates Root Protection, and Leaf Antioxidant Enzymes in Lead Stressed Rice Plants: Central Roles to Minimize Pb Content and Oxidative Stress. *Environ. Pollut.* **2021**, *280*, 116992. [CrossRef]
17. Pandey, A.K.; Zori, L.; Sun, T.; Karanovi, D.; Fang, P.; Borišev, M.; Wu, X.; Lukovi, J.; Xu, P. The Anatomical Basis of Heavy Metal Responses in Legumes and Their Impact on Plant—Rhizosphere Interactions. *Plants* **2022**, *11*, 2554. [CrossRef]
18. Altunkaynak, F.; Yalçin, E.; Çavuşoğlu, K. Assessment of Multifaceted Toxicity Induced by Heavy Metal Contamination in the Gelevera Stream Using the Allium Test. *Sci. Rep.* **2025**, *15*, 33037. [CrossRef]
19. Yadav, V.; Arif, N.; Kováč, J.; Singh, V.P.; Tripathi, D.K.; Chauhan, D.K.; Vaculík, M. Structural Modifications of Plant Organs and Tissues by Metals and Metalloids in the Environment: A Review. *Plant Physiol. Biochem.* **2021**, *159*, 100–112. [CrossRef] [PubMed]
20. Araniti, F.; Talarico, E.; Letizia, M.; Greco, E.; Minervino, M.; Alvarez-rodríguez, S.; Muto, A.; Ferrari, M.; Chiappetta, A.; Bruno, L. Short-Term Exposition to Acute Cadmium Toxicity Induces the Loss of Root Gravitropic Stimuli Perception through PIN2-Mediated Auxin Redistribution in *Arabidopsis thaliana* (L.) Heynh. *Plant Sci.* **2023**, *332*, 111726. [CrossRef] [PubMed]
21. Gálusová, T.; Piršelová, B.; Rybanský, Ľ.; Krasylenko, Y.; Mészáros, P.; Blehová, A.; Bardáčová, M.; Moravčíková, J.; Matušíková, I. Plasticity of Soybean Stomatal Responses to Arsenic and Cadmium at the Whole Plant Level. *Polish J. Environ. Stud.* **2020**, *29*, 3569–3580. [CrossRef]
22. Guo, Z.; Gao, Y.; Yuan, X.; Yuan, M.; Huang, L.; Wang, S.; Liu, C.; Duan, C. Effects of Heavy Metals on Stomata in Plants: A Review. *Int. J. Mol. Sci.* **2023**, *24*, 9302. [CrossRef]
23. Sadeghipour, O. Cadmium Toxicity Alleviates by Seed Priming with Proline or Glycine Betaine in Cowpea (*Vigna unguiculata* (L.) Walp.). *Egypt. J. Agron.* **2020**, *42*, 163–170. [CrossRef]
24. Khan, K.Y.; Ali, B.; Stoffell, P.J.; Cui, X.; Yang, X.; Guo, Y. Study Amino Acid Contents, Plant Growth Variables and Cell Ultrastructural Changes Induced by Cadmium Stress between Two Contrasting Cadmium Accumulating Cultivars of *Brassica rapa* ssp. *Chinensis* L. (Pak Choi). *Ecotoxicol. Environ. Saf.* **2020**, *200*, 110748. [CrossRef]
25. Chen, S.; Tang, Z.; Hou, J.; Gao, J.; Li, X.; Zhang, Y.; Zhao, Q. 2, 4-Epibrassinolide Mitigates Cd Stress by Enhancing Chloroplast Structural Remodeling and Chlorophyll Metabolism in *Vigna angularis* Leaves. *Biol. Trace Elem. Res.* **2025**, *14*, 674. [CrossRef]
26. Grajek, H.; Rydzynski, D.; Piotrowicz-Cieslak, A.; Herman, A.; Maciejczyk, M.; Wieczorek, Z. Cadmium Ion-Chlorophyll Interaction e Examination of Spectral Properties and Structure of the Cadmium-Chlorophyll Complex and Their Relevance to Photosynthesis Inhibition. *Chemosphere* **2020**, *261*, 127434. [CrossRef]
27. Yamatani, H.; Ito, T.; Nishimura, K.; Yamada, T.; Sakamoto, W.; Kusaba, M. Genetic Analysis of Chlorophyll Synthesis and Degradation Regulated by Balance of Chlorophyll Metabolism. *Plant Physiol.* **2022**, *189*, 419–432. [CrossRef] [PubMed]

28. Ghassemi-golezani, K.; Rahimzadeh, S. Foliar Spray of Carbon Quantum Dots Alleviated Cadmium Stress in *Dracocephalum moldavica* by Altering Physiological and Biochemical Responses. *Sci. Rep.* **2025**, *15*, 32325. [CrossRef] [PubMed]
29. Jia, L.; Yu, G.; Zhao, Z.; Lü, L. Effects of Cadmium (Cd) on Photosynthetic Characteristics and Chlorophyll Fluorescence Parameters in the Ornamental Plant *Salvia splendens* Ker-Gawl. *Physiol. Mol. Biol. Plants* **2025**, *31*, 507–519. [CrossRef]
30. Hou, L.; Ji, S.; Zhang, Y.; Wu, X.; Zhang, L.; Liu, P. The Mechanism of Silicon on Alleviating Cadmium Toxicity in Plants: A Review. *Front. Plant Sci.* **2023**, *14*, 1141138. [CrossRef]
31. Shabab, Z.; Sarada, D.L. 24-Epibrassinolide Mitigates Arsenate Stress in Seedlings of *Oryza sativa* (IR-20) via the Induction of Phenylpropanoid Pathway. *Plant Physiol. Biochem.* **2024**, *215*, 109023. [CrossRef] [PubMed]
32. Oh, M.H.; Honey, S.H.; Tax, F.E. The Control of Cell Expansion, Cell Division, and Vascular Development by Brassinosteroids: A Historical Perspective. *Int. J. Mol. Sci.* **2020**, *21*, 1743. [CrossRef]
33. Ali, M.M.; Anwar, R.; Malik, A.U.; Khan, A.S.; Ahmad, S.; Hussain, Z.; Hasan, M.U.; Mudassar, N.; Chen, F. Plant Growth and Fruit Quality Response of Strawberry Is Improved After Exogenous Application of 24—Epibrassinolide. *J. Plant Growth Regul.* **2021**, *41*, 1786–1799. [CrossRef]
34. Sheikhi, S.; Ebrahimi, A.; Heidari, P.; Amerian, M.R.; Rashidi-Monfared, S.; Alipour, H. Exogenous 24—Epibrassinolide Ameliorates Tolerance to High—Temperature by Adjusting the Biosynthesis of Pigments, Enzymatic, Non—Enzymatic Antioxidants, and Diosgenin Content in Fenugreek. *Sci. Rep.* **2023**, *13*, 6661. [CrossRef]
35. Piacentini, D.; Rovere, F.D.; Lanni, F.; Cittadini, M.; Palombi, M.; Fattorini, L.; Cecchetti, V.; Altamura, M.M.; Falasca, G. Brassinosteroids Interact with Nitric Oxide in the Response of Rice Root Systems to Arsenic Stress. *Environ. Exp. Bot.* **2023**, *209*, 105287. [CrossRef]
36. Huang, Q.; Zhang, Y.; Liu, S.; Wang, H.; Gao, F.; Shao, G. 24-Epibrassinolide Mitigates Cadmium Toxicity in Rice Plants by Activating the Plant Detoxification System and Regulating Genes Expression Involved in Cd/Fe Uptake and Translocation. *Plant Stress* **2024**, *12*, 100485. [CrossRef]
37. Wang, X.; Li, H.; Zhang, S.; Gao, F.; Sun, X.; Ren, X. Interactive Effect of 24-Epibrassinolide and Silicon on the Alleviation of Cadmium Toxicity in Rice (*Oryza sativa* L.) Plants. *Environ. Technol.* **2024**, *45*, 4725–4736. [CrossRef] [PubMed]
38. Shabab, Z.; Dronamraju, S.V.L. Induction of Brassinazole Resistant-1 upon Exogenous Application of 24-Epibrassinolide Enhances Arsenate Tolerance in *Oryza sativa* Seedlings. *Plant Physiol. Biochem.* **2025**, *227*, 110060. [CrossRef]
39. Ahmar, S.; Shafique, M.S.; Rapacz, M.; Pociecha, E. Elucidating the Role of Brassinosteroid Signaling Genes and Their Promoters in Arabidopsis Revealed Regulatory Mechanisms in Plant Development and Responses to Different Abiotic Stresses. *BMC Plant Biol.* **2025**, *25*, 970. [CrossRef]
40. He, Z.; Zhou, M.; Feng, X.; Di, Q.; Meng, D.; Yu, X.; Yan, Y.; Sun, M.; Li, Y. The Role of Brassinosteroids in Plant Cold Stress Response. *Life* **2024**, *14*, 1015. [CrossRef] [PubMed]
41. Silva, A.P.S.d.; Alencar, A.A.d.S.; Sudré, C.P.; Araújo, M.d.S.B.d.; Lobato, A.K.d.S. Brassinosteroids: Relevant Evidence Related to Mitigation of Abiotic and Biotic Stresses in Plants. *Agronomy* **2024**, *14*, 840. [CrossRef]
42. Khosravifar, F.; Mohammadi, M.; Eghlima, G. Brassinosteroids Improve Drought Resistance in Zinnia by Regulating Antioxidant Activity and Hormonal Interactions with ABA and Salicylic Acid. *Plant Growth Regul.* **2025**, *150*, 2259–2273. [CrossRef]
43. Balal, R.M.; Javed, S.A.; Jaffar, M.T.; Sadaf, A.; Paray, B.A.; Singh, R. Heavy Metal Toxicity Induced by Sewage Water Treatment in Three Different Vegetables (Lettuce, Spinach and Cabbage) Was Alleviated by Brassinosteroid and Silicon Supplementation. *J. King Saud Univ.—Sci.* **2024**, *36*, 103310. [CrossRef]
44. Kour, J.; Kohli, S.; Khanna, K.; Bakshi, P.; Sharma, P.; Singh, A.D.; Ibrahim, M.; Devi, K.; Sharma, N.; Ohri, P.; et al. Brassinosteroid Signaling, Crosstalk and Physiological Functions in Plants under Heavy Metal Stress. *Front. Plant Sci.* **2021**, *12*, 608061. [CrossRef]
45. Miao, R.; Li, C.; Liu, Z.; Zhou, X.; Chen, S.; Zhang, D.; Luo, J.; Tang, W.; Wang, C.; Wu, J.; et al. The Role of Endogenous Brassinosteroids in the Mechanisms Regulating Plant Reactions to Various Abiotic Stresses. *Agronomy* **2024**, *14*, 356. [CrossRef]
46. Usmani, L.; Shakil, A.; Khan, I.; Alvi, T.; Singh, S.; Das, D. Brassinosteroids in Micronutrient Homeostasis: Mechanisms and Implications for Plant Nutrition and Stress Resilience. *Plants* **2025**, *14*, 598. [CrossRef]
47. Shaghaleh, H.; Hamoud, Y.A.; Saleem, M.H.; Elansary, H.O.; Mahmoud, E.A.; Sheteiwy, M.S. Phytohormonal Modulation Alleviates Arsenic Toxicity in Rice by Enhancing Antioxidant Defenses, Proline Metabolism, and Arsenic Detoxification Mechanisms. *Sci. Rep.* **2025**, *15*, 26953. [CrossRef]
48. Sun, J.Y.; Guo, R.; Jiang, Q.; Chen, C.Z.; Gao, Y.Q.; Jiang, M.M.; Shen, R.F.; Zhu, X.F.; Huang, J. Brassinosteroid Decreases Cadmium Accumulation via Regulating Gibberellic Acid Accumulation and Cd Fixation Capacity of Root Cell Wall in Rice (*Oryza sativa*). *J. Hazard. Mater.* **2024**, *469*, 133862. [CrossRef] [PubMed]
49. Niu, K.; Xiao, H.; Wang, Y.; Cui, T.; Zhao, C. A Meta-Analysis on Plant Growth and Heavy Metals Uptake with the Application of 2,4-Epibrassinolide in Contaminated Soils. *Ecotoxicol. Environ. Saf.* **2025**, *289*, 117439. [CrossRef]
50. Talarek-karwel, M.; Bajguz, A.; Piotrowska-Niczyporuk, A. 24-Epibrassinolide Modulates Primary Metabolites, Antioxidants, and Phytochelatins in *Acutodesmus obliquus* Exposed to Lead Stress. *J. Appl. Phycol.* **2020**, *32*, 263–276. [CrossRef]

51. Sehrish, A.K.; Ahmad, S.; Ali, S.; Tabssam, R.; Ai, F.; Du, W.; Guo, H. Alleviation of Cadmium Toxicity by Improving Antioxidant Defense Mechanism and Nutrient Uptake in Wheat (*Triticum aestivum* L.) through Foliar Application of 24-Epibrassinolide under Elevated CO_2. *J. Hazard. Mater.* **2024**, *480*, 136209. [CrossRef]
52. Jan, S.; Alyemeni, M.N.; Wijaya, L.; Alam, P.; Siddique, K.H.; Ahmad, P. Interactive Effect of 24-Epibrassinolide and Silicon Alleviates Cadmium Stress via the Modulation of Antioxidant Defense and Glyoxalase Systems and Macronutrient Content in *Pisum sativum* L. Seedlings. *BMC Plant Biol.* **2018**, *18*, 146. [CrossRef] [PubMed]
53. Nolan, T.M.; Vukasinović, N.; Liu, D.; Russinova, E.; Yin, Y. Brassinosteroids: Multidimensional Regulators of Plant Growth, Development, and Stress Responses. *Plant Cell* **2020**, *32*, 298–318. [CrossRef]
54. Dong, F.; Li, X.; Liu, C.; Zhao, B.; Ma, Y.; Ji, W. Exogenous 24-Epibrassinolide Mitigates Damage in Grape Seedlings under Low-Temperature Stress. *Front. Plant Sci.* **2025**, *16*, 1487680. [CrossRef]
55. Nirmalaruban, R.; Yadav, R.; Sugumar, S.; Alekya, M.; Mazumder, A.K.; Babu, P.; Kumar, M.; Gaikwad, K.B.; Bainsla, N.K.; Singh, S.K.; et al. Rooting for Resilience: Central Metaxylem Area as a Breeding Target for Yield Gain and Resilience in Wheat (*Triticum aestivum* L.). *BMC Plant Biol.* **2025**, *25*, 493. [CrossRef]
56. Sousa, V.Q.; Messias, W.F.S.; Pereira, Y.C.; da Silva, B.R.S.; Lobato, E.M.S.G.; Alyemeni, M.N.; Ahmad, P.; Lobato, A.K.d.S. Pretreatment with 24-Epibrassinolide Synergistically Protects Root Structures and Chloroplastic Pigments and Upregulates Antioxidant Enzymes and Biomass in Na^+-Stressed Tomato Plants. *J. Plant Growth Regul.* **2021**, *41*, 2869–2885. [CrossRef]
57. Gupta, P.; Seth, C.S. 24-Epibrassinolide Regulates Functional Components of Nitric Oxide Signalling and Antioxidant Defense Pathways to Alleviate Salinity Stress in *Brassica juncea* L. Cv. Varuna. *J. Plant Growth Regul.* **2022**, *42*, 4207–4222. [CrossRef]
58. Lv, Z.; Zhao, W.; Kong, S.; Li, L.; Lin, S. Overview of Molecular Mechanisms of Plant Leaf Development: A Systematic Review. *Front. Plant Sci.* **2023**, *14*, 1293424. [CrossRef] [PubMed]
59. Javelle, M.; Vernoud, V.; Rogowsky, P.M.; Ingram, G.C. Epidermis: The Formation and Functions of a Fundamental Plant Tissue. *New Phytol.* **2011**, *189*, 17–39. [CrossRef] [PubMed]
60. Salam, A.; Chang, J.; Yang, L.; Zeeshan, M.; Iqbal, A.; Khan, A.R.; Afridi, M.S.; Ulhassan, Z.; Azhar, W.; Zhang, Z.; et al. Brassinosteroid-Mediated Resistance to Cobalt-Induced Toxicity by Regulating Hormonal Balance, Cellular Metabolism, and Antioxidant Defense in Maize. *Plants* **2025**, *14*, 2076. [CrossRef]
61. Santos, L.A.; Silva, B.R.S.; Lobato, A.K.S. Foliar-Applied 24-Epibrassinolide Systemically Triggers Tolerance to Magnesium Stress in Soybean Plants: Plausible Responses Focused on Root and Leaf Structures. *Bot. Lett.* **2021**, *168*, 558–569. [CrossRef]
62. Magota, K.; Gotoh, E.; Sakaguchi, S.; Ikeda, H.; Setoguchi, H. High-Intensity Light Promotes Adaptive Divergence of Photosynthetic Traits between Sun-Exposed and Shaded Populations in *Saxifraga fortunei*. *Am. J. Bot.* **2024**, *111*, e16371. [CrossRef]
63. Peduzzi, A.; Piacentini, D.; D'Angeli, S.; Iozia, L.M.; Varone, L.; Amato, F.; Altamura, M.M.; Falasca, G. Brassinosteroid Seed Priming Positively Affects Leaf Anatomy and Gas Exchanges in a Salt-Sensitive Sorghum Genotype Exposed to Salt Stress. *Plant Stress* **2025**, *18*, 101014. [CrossRef]
64. Pereira-Matos, Y.C.; Lima, E.J.d.F.; Ribeiro, A.T.; Lange, C.N.; Batista, B.L.; El-Beltagi, H.S.; Bajguz, A.; Lobato, A.K.d.S. Exogenous 24-Epibrassinolide Reverses Disturbances in Zinc-Stressed Tomato by Synergistically Stimulating Leaf Structures, Photosynthesis and Growth. *S. Afr. J. Bot.* **2023**, *159*, 447–460. [CrossRef]
65. Park, T.-K.; Lee, S.-H.; Kim, S.-H.; Ko, Y.-W.; Oh, E.; Kim, Y.J.; Kim, T.-W. Dual Regulation of Stomatal Development by Brassinosteroid in Arabidopsis Hypocotyls. *J. Integr. Plant Biol.* **2025**, *67*, 258–275. [CrossRef]
66. Li, S.; Yan, J.; Chen, L.G.; Meng, G.; Zhou, Y.; Wang, C.M.; Jiang, L.; Luo, J.; Jiang, Y.; Li, Q.F.; et al. Brassinosteroid Regulates Stomatal Development in Etiolated Arabidopsis Cotyledons via Transcription Factors BZR1 and BES1. *Plant Physiol.* **2024**, *195*, 1382–1400. [CrossRef] [PubMed]
67. Wang, C.; Cui, H.; Jin, M.; Wang, J.; Li, C.; Li, Y.; Luo, Y.L.; Wang, Z. Enhancement of Wheat Resistance to Dry–Hot Wind Stress during Grain Filling by 24-Epibrassinolide: Optimization of Hormone Balance and Improvement of Flag Leaf Photosynthetic Performance. *Front. Plant Sci.* **2025**, *16*, 1552617. [CrossRef] [PubMed]
68. Maia, C.F.; Pereira, Y.C.; Silva, B.R.S.; Batista, B.L.; Lobato, A.K.S. Exogenously Applied 24-Epibrassinolide Favours Stomatal Performance, ROS Detoxification and Nutritional Balance, Alleviating Oxidative Damage Against the Photosynthetic Apparatus in Tomato Leaves Under Nickel Stress. *J. Plant Growth Regul.* **2023**, *42*, 2196–2211. [CrossRef]
69. Martins, J.P.R.; Santos, E.R.; Rodrigues, L.C.A.; Gontijo, A.B.P.L.; Falqueto, A.R. Effects of 6-Benzylaminopurine on Photosystem II Functionality and Leaf Anatomy of in Vitro Cultivated Aechmea Blanchetiana. *Biol. Plant.* **2018**, *62*, 793–800. [CrossRef]
70. Camargo, M.A.B.; Marenco, R.A. Density, Size and Distribution of Stomata in 35 Rainforest Tree Species in Central Amazonia. *Acta Amaz.* **2011**, *41*, 205–212. [CrossRef]
71. Vráblová, M.; Vrábl, D.; Hronková, M.; Kubásek, J.; Šantrůček, J. Stomatal Function, Density and Pattern, and CO_2 Assimilation in *Arabidopsis thaliana* Tmm1 and Sdd1-1 Mutants. *Plant Biol.* **2017**, *19*, 689–701. [CrossRef]
72. Prestes, L.R.; Silva, M.M.S.; Silva, S.G.A.; Gonçalves, M.A.F.; Batista, B.L.; Viana, I.B.; Lobato, A.K.d.S. Dopamine and 24-Epibrassinolide Upregulate Root Resilience, Mitigating Lead Stress on Leaf Tissue and Stomatal Performance in Tomato Plants. *Agronomy* **2025**, *15*, 239. [CrossRef]

73. Lobato, A.K.d.S.; Pontes, C.V.S.; Gonçalves, M.A.F.; Santos, V.C.d.; Carvalho, N.C.F.d.; Ferreira, T.d.S.; Lopes, L.K.C.; Silva, B.R.S.d. Chloroplast Damage Induced by Simulated Acid Rain Is Delayed in Soybean Plants Pretreated with 24-Epibrassinolide. *Plant Biosyst.* **2025**, *159*, 419–430. [CrossRef]
74. Siddiqui, H.; Ahmed, K.B.M.; Sami, F.; Hayat, S. Phytoremediation of Cadmium Contaminated Soil Using *Brassica juncea*: Influence on PSII Activity, Leaf Gaseous Exchange, Carbohydrate Metabolism, Redox and Elemental Status. *Bull. Environ. Contam. Toxicol.* **2020**, *105*, 411–421. [CrossRef] [PubMed]
75. Deng, X.G.; Zhu, T.; Peng, X.J.; Xi, D.H.; Guo, H.; Yin, Y.; Zhang, D.W.; Lin, H.H. Role of Brassinosteroid Signaling in Modulating *Tobacco mosaic virus* Resistance in *Nicotiana benthamiana*. *Sci. Rep.* **2016**, *6*, 20579. [CrossRef]
76. Luo, P.; Wu, J.; Li, T.T.; Shi, P.; Ma, Q.; Di, D.W. An Overview of the Mechanisms through Which Plants Regulate ROS Homeostasis under Cadmium Stress. *Antioxidants* **2024**, *13*, 1174. [CrossRef]
77. Sharma, D.; Bhardwaj, S.; Raza, A.; Singh, R.; Kapoor, D.; Sharma, N.R.; Prasad, P.V.V. Alleviatory Effects of Silicon and 24-Epibrassinolide in Modulation of Growth, Osmolytes, Metabolites, Antioxidant Defense System, and Gene Expression in Lead-Exposed Fenugreek (*Trigonella foenum-graecum* L.) Plants. *Agronomy* **2023**, *13*, 1884. [CrossRef]
78. Saraiva, M.P.; Maia, C.F.; Batista, B.L.; Lobato, A.K.d.S. Ionic Homeostasis and Redox Metabolism Upregulated by 24-Epibrassinolide Are Crucial for Mitigating Nickel Excess in Soybean Plants, Enhancing Photosystem II Efficiency and Biomass. *Plant Biol.* **2022**, *25*, 343–355. [CrossRef] [PubMed]
79. Ayyaz, A.; Farooq, M.A.; Dawood, M.; Majid, A.; Javed, M.; Athar, H.-R.; Bano, H.; Zafar, Z.U. Exogenous Melatonin Regulates Chromium Stress-Induced Feedback Inhibition of Photosynthesis and Antioxidative Protection in Brassica Napus Cultivars. *Plant Cell Rep.* **2021**, *40*, 2063–2080. [CrossRef]
80. Yang, H.; Zhao, J.; Yin, X.; Ding, K.; Gao, X.; Cai, Y.; Pan, Y.; Jiang, B.; Liu, Q.; Jia, Y. Mitigating Ni and Cu Ecotoxicity in the Ecological Restoration Material and Ornamental Primula Forbesii Franch. with Exogenous 24-Epibrassinolide and Melatonin. *Sci. Rep.* **2024**, *14*, 16067. [CrossRef]
81. Basit, F.; Tao, J.; An, J.; Song, X.; Sheteiwy, M.S.; Holford, P.; Hu, J.; Jośko, I.; Guan, Y. Nitric Oxide and Brassinosteroids Enhance Chromium Stress Tolerance in *Glycine max* L. (Merr.) by Modulating Antioxidative Defense and Glyoxalase Systems. *Environ. Sci. Pollut. Res.* **2023**, *30*, 51638–51653. [CrossRef]
82. Liu, X.; Zhu, Q.; Liu, W.; Zhang, J. 24-Epibrassinolide Confers Zinc Stress Tolerance in Watermelon Seedlings through Modulating Antioxidative Capacities and Lignin Accumulation. *PeerJ* **2023**, *11*, e15330. [CrossRef] [PubMed]
83. Fan, P.; Wu, L.; Wang, Q.; Wang, Y.; Luo, H.; Song, J.; Yang, M.; Yao, H.; Chen, S. Physiological and Molecular Mechanisms of Medicinal Plants in Response to Cadmium Stress: Current Status and Future Perspective. *J. Hazard. Mater.* **2023**, *450*, 131008. [CrossRef]
84. Nie, W.; He, Q.; Ma, J.; Guo, H.; Shi, Q. Exogenous 2,4-Epibrassinolide Alleviates Alkaline Stress in Cucumber by Modulating Photosynthetic Performance. *Plants* **2025**, *14*, 54. [CrossRef]
85. Dong, Y.; Chen, W.; Bai, X.; Liu, F.; Wan, Y. Effects of Exogenous Nitric Oxide and 24-Epibrassinolide on the Physiological Characteristics of Peanut Seedlings Under Cadmium Stress. *Pedosphere* **2019**, *29*, 45–59. [CrossRef]
86. Shafi, Z.; Shahid, M.; AlGarawi, A.M.; Zeyad, M.T.; Marey, S.A.; Hatamleh, A.A.; Wang, S.; Singh, U.B. The Exogenous Application of 24-Epibrassinolide (24-EBL) Increases the Cd and Pb Resilience in *Zea mays* (L.) by Regulating the Growth and Physiological Mechanism. *Appl. Biochem. Biotechnol.* **2023**, *196*, 3949–3973. [CrossRef]
87. Guo, Y.Y.; Tian, S.S.; Liu, S.S.; Wang, W.Q.; Sui, N. Energy Dissipation and Antioxidant Enzyme System Protect Photosystem II of Sweet Sorghum under Drought Stress. *Photosynthetica* **2018**, *56*, 861–872. [CrossRef]
88. Meng, C.; Sui, N. Overexpression of Maize MYB-IF35 Increases Chilling Tolerance in Arabidopsis. *Plant Physiol. Biochem.* **2019**, *135*, 167–173. [CrossRef] [PubMed]
89. Liang, C.; Ge, Y.; Su, L.; Bu, J. Response of Plasma Membrane H+-ATPase in Rice (*Oryza sativa*) Seedlings to Simulated Acid Rain. *Environ. Sci. Pollut. Res.* **2015**, *22*, 535–545. [CrossRef] [PubMed]
90. Lima, M.D.R.; Barros Junior, U.O.; Batista, B.L.; Lobato, A.K.S. Brassinosteroids Mitigate Iron Deficiency Improving Nutritional Status and Photochemical Efficiency in *Eucalyptus urophylla* Plants. *Trees* **2018**, *32*, 1681–1694. [CrossRef]
91. Zhao, X.Q.; Shi, J.; Niu, Y.N.; Lu, P.N.; Chen, X.J.; Mao, T.T. 24-Epibrassinolide Alleviates Aluminum Toxicity by Improving Leaf Chlorophyll Fluorescence and Photosynthetic Performance and Root Antioxidant-Oxidant Balance and Ascorbate-Glutathione Cycle in Maize. *Russ. J. Plant Physiol.* **2022**, *69*, 99. [CrossRef]
92. dos Santos, L.R.; Paula, L.d.S.; Pereira, Y.C.; da Silva, B.R.S.; Batista, B.L.; Alsahli, A.A.; Lobato, A.K.d.S. Brassinosteroids-Mediated Amelioration of Iron Deficiency in Soybean Plants: Beneficial Effects on the Nutritional Status, Photosynthetic Pigments and Chlorophyll Fluorescence. *J. Plant Growth Regul.* **2021**, *40*, 1803–1823. [CrossRef]
93. Zhou, R.; Xu, J.; Li, L.; Yin, Y.; Xue, B.; Li, J.; Sun, F. Exploration of the Effects of Cadmium Stress on Photosynthesis in *Oenanthe javanica* (Blume) DC. *Toxics* **2024**, *12*, 307. [CrossRef] [PubMed]
94. Chu, J.; Zhu, F.; Chen, X.; Liang, H.; Wang, R.; Wang, X.; Huang, X. Effects of Cadmium on Photosynthesis of Schima Superba Young Plant Detected by Chlorophyll Fluorescence. *Environ. Sci. Pollut. Res.* **2018**, *25*, 10679–10687. [CrossRef]

95. Li, J.; Yang, P.; Gan, Y.; Yu, J.; Xie, J. Brassinosteroid Alleviates Chilling-Induced Oxidative Stress in Pepper by Enhancing Antioxidation Systems and Maintenance of Photosystem II. *Acta Physiol. Plant.* **2015**, *37*, 222. [CrossRef]
96. Zhao, M.; Yuan, L.; Wang, J.; Xie, S.; Zheng, Y.; Nie, L.; Zhu, S.; Hou, J.; Chen, G.; Wang, C. Transcriptome Analysis Reveals a Positive Effect of Brassinosteroids on the Photosynthetic Capacity of Wucai under Low Temperature. *BMC Genom.* **2019**, *20*, 810. [CrossRef]
97. Hu, W.H.; Hu, X.H.; Liu, C.; Wang, B.Q.; Yan, X.H. 24-Epibrassinolide Improved Chilled Tomato Photosynthetic Performance by Stabilizing Electron Transport Chain and Function of Photosystem II. *Biol. Plant.* **2022**, *66*, 178–187. [CrossRef]
98. Alam, P.; Kohli, S.K.; Al Balawi, T.; Altalayan, F.H.; Alam, P.; Ashraf, M.; Bhardwaj, R.; Ahmad, P. Foliar Application of 24-Epibrassinolide Improves Growth, Ascorbate-Glutathione Cycle, and Glyoxalase System in Brown Mustard (*Brassica juncea* (L.) Czern.) under Cadmium Toxicity. *Plants* **2020**, *9*, 1487. [CrossRef]
99. Li, B.B.; Fu, Y.S.; Li, X.X.; Yin, H.N.; Xi, Z.M. Brassinosteroids Alleviate Cadmium Phytotoxicity by Minimizing Oxidative Stress in Grape Seedlings: Toward Regulating the Ascorbate-Glutathione Cycle. *Sci. Hortic.* **2022**, *299*, 111002. [CrossRef]
100. Fariduddin, Q.; Yusuf, M.; Ahmad, I.; Ahmad, A. Brassinosteroids and Their Role in Response of Plants to Abiotic Stresses. *Biol. Plant.* **2014**, *58*, 9–17. [CrossRef]
101. da Silva Bezerra, L.B.; Viana, A.P.; de Paula Bernado, W.; Mendes, D.S.; Campostrini, E.; da Silva, F.A. Viral Infection by CABMV-Cowpea Aphid-Borne Mosaic Virus- Reduces Gas Exchange in Passion Fruit Leaves. *Eur. J. Plant Pathol.* **2025**, *172*, 105–121. [CrossRef]
102. Amarasinghe, R.M.N.T.; Sakimin, S.Z.; Megat Wahab, P.E.; Ramlee, S.I.; Nakasha, J.J. Frequency of Application of 24-Epibrassinolide on Plant Growth, Physiology and Postharvest Fruit Quality of Cantaloupe Grown at Elevated Temperature. *Int. J. Veg. Sci.* **2023**, *29*, 358–374. [CrossRef]
103. Pereira, Y.C.; Nascimento, A.N.S.; Aguiar, B.T.S.; Silva, B.R.S.; Barbosa, M.A.M.; Batista, B.L.; Bajguz, A.; Lobato, A.K.S. Anatomical Modifications Modulated by Pretreatment with 24—Epibrassinolide Alleviate Boron Stress in Soybean Plants: Valuable Repercussions on Nutrient Contents, Photosynthesis, and Biomass. *J. Soil Sci. Plant Nutr.* **2022**, *22*, 4533–4550. [CrossRef]
104. Cruzado-Tafur, E.; Orzoł, A.; Gołębiowski, A.; Pomastowski, P.; Cichorek, M.; Olszewski, J.; Walczak-Skierska, J.; Buszewski, B.; Szultka-Młyńska, M.; Głowacka, K. Metal Tolerance and Cd Phytoremoval Ability in *Pisum sativum* Grown in Spiked Nutrient Solution. *J. Plant Res.* **2023**, *136*, 931–945. [CrossRef]
105. Soni, S.; Jha, A.B.; Dubey, R.S.; Sharma, P. Mitigating Cadmium Accumulation and Toxicity in Plants: The Promising Role of Nanoparticles. *Sci. Total Environ.* **2024**, *912*, 168826. [CrossRef]
106. Jin, Y.; Yang, P.; Li, J.; Yang, Y.; Yang, R.; Fu, H.; Li, J. Brassinosteroids Alleviate Salt Stress by Enhancing Sugar and Glycine Betaine in Pepper (*Capsicum annuum* L.). *Plants* **2024**, *13*, 3029. [CrossRef] [PubMed]
107. Ribeiro, D.M.; Santos, S.d.N.B.d.; Ferreira, D.C.d.S.; Miranda, J.F.F.d.; Oliveira, J.T.d.; Cunha, F.F.d.; Velloso, C.L.A.d.P.; Silva, P.A.; Oliveira Neto, C.F.d. Effect of 24-Epibrassinolide Plant Hormone Rates on the Level of Macronutrients in Forage Sorghum Plants Subjected to Water Deficit and Rehydration. *Grasses* **2025**, *4*, 33. [CrossRef]
108. Haider, F.U.; Zulfiqar, U.; Noor-ul-Ain; Mehmood, T.; Shahzad, B.; Cao, L.; Yong, J.W.H.; Binobead, M.A. Effects of Titanium Oxide Nanoparticles and 24-Epibrassinosteroid to Mitigate the Toxicity of Cadmium (Cd) and Improve Physio-Morphological Traits of Soybean (*Glycine max* L.) Cultivated under Cd-Contaminated Soil. *Environ. Technol. Innov.* **2024**, *36*, 103811. [CrossRef]
109. Lima, J.V.; Lobato, A.K.S. Brassinosteroids Improve Photosystem II Efficiency, Gas Exchange, Antioxidant Enzymes and Growth of Cowpea Plants Exposed to Water Deficit. *Physiol. Mol. Biol. Plants* **2017**, *23*, 59–72. [CrossRef]
110. Pereira, Y.C.; Rodrigues, W.S.; Lima, E.J.A.; Santos, L.R.; Silva, M.H.L.; Lobato, A.K.S. Brassinosteroids Increase Electron Transport and Photosynthesis in Soybean Plants under Water Deficit. *Photosynthetica* **2019**, *57*, 181–191. [CrossRef]
111. Ahammed, G.J.; Choudhary, S.P.; Chen, S.; Xia, X.; Shi, K.; Zhou, Y.; Yu, J. Role of Brassinosteroids in Alleviation of Phenanthrene–Cadmium Co-Contamination-Induced Photosynthetic Inhibition and Oxidative Stress in Tomato. *J. Exp. Bot.* **2013**, *64*, 199–213. [CrossRef]
112. Santos, L.R.; Batista, B.L.; Lobato, A.K.S. Brassinosteroids Mitigate Cadmium Toxicity in Cowpea Plants. *Photosynthetica* **2018**, *56*, 591–605. [CrossRef]
113. Paniz, F.P.; Pedron, T.; Freire, B.M.; Torres, D.P.; Silva, F.F.; Batista, B.L. Effective Procedures for the Determination of As, Cd, Cu, Fe, Hg, Mg, Mn, Ni, Pb, Se, Th, Zn, U and Rare Earth Elements in Plants and Foodstuffs. *Anal. Methods* **2018**, *10*, 4094–4103. [CrossRef]
114. Lobato, A.K.S.; Barbosa, M.A.M.; Alsahli, A.A.; Lima, E.J.A.; Silva, B.R.S. Exogenous Salicylic Acid Alleviates the Negative Impacts on Production Components, Biomass and Gas Exchange in Tomato Plants under Water Deficit Improving Redox Status and Anatomical Responses. *Physiol. Plant.* **2021**, *172*, 869–884. [CrossRef]
115. O'Brien, T.P.; Feder, N.; McCully, M.E. Polychromatic Staining of Plant Cell Walls by Toluidine Blue O. *Protoplasma* **1964**, *59*, 368–373. [CrossRef]
116. Segatto, F.B.; Bisognin, D.A.; Benedetti, M.; Costa, L.C.; Rampelotto, M.V.; Nicoloso, F.T. A Technique for the Anatomical Study of Potato Leaf Epidermis. *Cienc. Rural* **2004**, *34*, 1597–1601. [CrossRef]

117. Badawi, G.H.; Yamauchi, Y.; Shimada, E.; Sasaki, R.; Kawano, N.; Tanaka, K.; Tanaka, K. Enhanced Tolerance to Salt Stress and Water Deficit by Overexpressing Superoxide Dismutase in Tobacco (*Nicotiana tabacu*) Chloroplasts. *Plant Sci.* **2004**, *166*, 919–928. [CrossRef]
118. Giannopolitis, C.N.; Ries, S.K. Superoxide Dismutases: I. Occurrence in Higher Plants. *Plant Physiol.* **1977**, *59*, 309–314. [CrossRef]
119. Havir, E.A.; McHale, N.A. Biochemical and Developmental Characterization of Multiple Forms of Catalase in Tobacco Leaves. *Plant Physiol.* **1987**, *84*, 450–455. [CrossRef] [PubMed]
120. Nakano, Y.; Asada, K. Hydrogen Peroxide Is Scavenged by Ascorbate-Specific Peroxidase in Spinach Chloroplasts. *Plant Cell Physiol.* **1981**, *22*, 867–880. [CrossRef]
121. Cakmak, I.; Marschner, H. Magnesium Deficiency and High Light Intensity Enhance Activities of Superoxide Dismutase, Ascorbate Peroxidase, and Glutathione Reductase in Bean Leaves. *Plant Physiol.* **1992**, *98*, 1222–1227. [CrossRef]
122. Elstner, E.F.; Heupel, A. Inhibition of Nitrite Formation from Hydroxylammoniumchloride: A Simple Assay for Superoxide Dismutase. *Anal. Biochem.* **1976**, *70*, 616–620. [CrossRef]
123. Bradford, M.M. A Rapid and Sensitive Method for the Quantitation of Microgram Quantities of Protein Utilizing the Principle of Protein-Dye Binding. *Anal. Biochem.* **1976**, *72*, 248–254. [CrossRef] [PubMed]
124. Wu, Q.-S.; Xia, R.-X.; Zou, Y.-N. Reactive Oxygen Metabolism in Mycorrhizal and Non-Mycorrhizal Citrus (Poncirus Trifoliata) Seedlings Subjected to Water Stress. *J. Plant Physiol.* **2006**, *163*, 1101–1110. [CrossRef]
125. Velikova, V.; Yordanov, I.; Edreva, A. Oxidative Stress and Some Antioxidant Systems in Acid Rain-Treated Bean Plants Protective Role of Exogenous Polyamines. *Plant Sci.* **2000**, *151*, 59–66. [CrossRef]
126. Cakmak, I.; Horst, W.J. Effect of Aluminium on Lipid Peroxidation, Superoxide Dismutase, Catalase, and Peroxidase Activities in Root Tips of Soybean (*Glycine max*). *Physiol. Plant.* **1991**, *83*, 463–468. [CrossRef]
127. Gong, M.; Li, Y.-J.; Chen, S.-Z. Abscisic Acid-Induced Thermotolerance in Maize Seedlings Is Mediated by Calcium and Associated with Antioxidant Systems. *J. Plant Physiol.* **1998**, *153*, 488–496. [CrossRef]
128. Lichtenthaler, H.K.; Buschmann, C. Chlorophylls and Carotenoids: Measurement and Characterization by UV-VIS Spectroscopy. In *Current Protocols in Food Analytical Chemistry*; John Wiley & Sons, Inc.: Hoboken, NJ, USA, 2001; pp. 431–438.
129. Steel, R.G.; Torrie, J.H.; Dickey, D.A. *Principles and Procedures of Statistics: A Biometrical Approach*, 3rd ed.; Academic Internet Publishers: Moorpark, CA, USA, 2006.
130. Venables, W.N.; Smith, D.M.; R Core Team. *An Introduction to R 2021*; R Core Team: Vienna, Austria, 2021; 105p.

Disclaimer/Publisher's Note: The statements, opinions and data contained in all publications are solely those of the individual author(s) and contributor(s) and not of MDPI and/or the editor(s). MDPI and/or the editor(s) disclaim responsibility for any injury to people or property resulting from any ideas, methods, instructions or products referred to in the content.